Archive

MASSACHUSETTS INSTITUTE OF TECHNOLOGY

THE ENERGY LABORATORY

AN ULTRASONIC FLOWMETER FOR GASES

by

Donald A. Bender
Leon R. Glicksman
Carl R. Peterson

Energy Laboratory
Report No. MIT-EL 84-020

October 1984

An Ultrasonic Flowmeter For Gases

by

Donald A. Bender

Submitted to the Department of Mechanical Engineering on October 15, 1982 in partial fulfillment of the requirements for the degree of Master of Science in Mechanical Engineering.

Abstract

An ultrasonic flowmeter is developed for use in natural gas mains. The characteristics of the application and the dynamic head device presently employed are described. The performance requirements, design, and prototype testing of the ultrasonic instrument are discussed. The viability of a unique metering technique using reflected acoustic pulses was experimentally demonstrated. The flowmeter developed herein requires access to one side of the gas line and is self calibrating. It was concluded that continued development will produce a unit suitable for use in commercial service.

Thesis Supervisor: Carl R. Peterson
Title: Associate Professor

Thesis Supervisor: Leon Glicksman
Title: Senior Scientist

Acknowledgements

I would like to thank Carl Peterson for sharing with me his vast wealth of insights and ideas, and for teaching me much of what I know about self motivation. I would like to thank Leon Glicksman for his patience, encouragement, and advice.

Thanks are due to Consolidated Edison for their financial support of this project. Thanks also go to the staff of Tiny's cage for helping me get things done.

I am grateful to the students of office 3-070 for serving as a whetstone against which I honed my wit. Finally, I am most grateful for my acquaintance with people and projects that had nothing to do with M.I.T. for helping me retain a perspective on what is known around here as *the real world.*

Table of Contents

List of Figures

List of Tables

Chapter 1
Introduction

Interdistrict flow measurements are presently made at seven points in the Consolidated Edison gas distribution network. These measurements indicate the total flow into the various sales districts. The total flow into each district is compared to the total sales of the district. A discrepancy indicates theft or leakage occuring in the district. It is necessary to measure these large volume flows accurately. The measurement points are located in a densely populated urban area and are accessible only through excavation. It is important to minimize the extent of the excavation by requiring that access to the line be limited to a short section of the upper portion of the line. It is also important to avoid interuptions to service.

The project encompassed by this thesis is the first phase of a development program that is to produce a flowmeter of high accuracy and reliability for use in measuring these interdistrict flows. Sections of this work are intended to serve as a design guide for the continuation of this program.

The highly specialized nature of this problem creates a number of constraints unique to this application. Among these constraints are the requirements of installation by insertion into a live main and a priori calibration. These restrictions are discussed in the following chapter on performance requirements.

A dynamic head device, the Annubar, manufactured by Deitrich Standard, is presently employed for these flow measurements. This device exhibits several characteristics which indicate limitations of its accuracy and reliability. First, the Annubar performs predictably only for well developed turbulent flow without swirl [13]. Second, the 3.5:1 useful range of this unit is relatively narrow [2]. Accuracy at low flow rates is limited. Finally, the device is

sensitive to fouling by particles entrained in the gas stream. The design and operation of the Annubar are discussed in Appendix A.

At the outset of this project, many flow measurement techniques were considered. Some of the concepts considered are listed in Table 1-I.

1. Alternate acoustic methods: Ultrasonoic technology using direct pulses or tonebursts.
2. Internally assembled turbine meter: Turbine meter using dual rotors assembled through a small opening in the line.
3. Laminar flow elements: Flow is divided so that regime becomes laminar. Pressure drop is measured.
4. Pressure drop over a known length: Differential pressure meter is used to measure pressure drop over several hundred foot length of pipe.
5. Pitot tube array: Sample dynamic head at many points.
6. Temperature effects due to compressibility: Use flow restrictions to induce pressure drop. Measure associated temperature change.
7. Variable diameter orifice plate: Orifice varies area to maintain a constant pressure drop.
8. Hot wire anemometer array: Sample velocity at many points.

Table 1-I: Candidate Flow Measurement Concepts

High accuracy requirements and the difficulty of implementing sophisticated mechanical design arising from geometric restrictions led to the elimination of many purely mechanical devices from consideration. Several other alternatives were found to be ineffective in meeting the desired performance goals. The most promising candidate concepts were the internally assembled turbine meter and ultrasonic techniques. While some other methods also showed potential for high accuracy, the internally assembled turbine meter and ultrasonic approaches were the most feasible. These approaches are discussed in Appendix B. Brief descriptions of the other alternative concepts are also presented in Appendix B. Ultrasonic technology was selected for development on the basis of its mechanical simplicity and potential for higher accuracy.

Research on the various aspects of ultrasonic flowmetering was conducted. A computer aided literature search yielded 259 pertinent references. Of these, 66 were directly applicable to the problem. These references provided a thorough insight into the state of the art of ultrasonic flowmetering technology. Prior art in ultrasonic flowmetering exists for large volume water measurement [12], ocean boundary layer studies [23], and gas flow measurement [17], [19]. It was found that meters having typical error of less than 1% of reading over a 25:1 flow range have been developed for related applications. A heretofore undeveloped approach based on the use of reflected shock pulses was pursued. This approach provides the high levels of performance that can be achieved through the use of ultrasonic technology while meeting the special requirements of this application. A technique by which the flowmeter can calibrate itself periodically and automatically was also developed.

Chapter 2

Performance Requirements

The flowmeter application discussed in this thesis places a variety of demands and limitations on whatever device is selected. The requirements may be divided into three categories: constraints imposed by the operating environment, functional requirements determined by the nature of the application, and performance goals in terms of the desired accuracy.

2.1 Service Environment

It is ultimately intended that a prototype be developed for installation at the Nereid and Wilder Ave annubar metering station [8]. The Nereid and Wilder station was selected by Consolidated Edison as being representative of the application. Specifications for the device developed herein are based on information from this point. The diameter at this location is 24 inches. The static pressure of the line will vary somewhat but is typically 160 psig. Flows up to an average maximum velocity of 30 feet per second are to be measured and reversals in flow direction will be encountered [7].

The ultrasonic flowmeter must be sufficiently flexible for use in various installations. Flow conditions will vary unpredictably between different locations. The weakness of fluid shear forces in gas results in the persistence of swirl at great distances from its source. Wall disturbances may produce an asymetric velocity distribution. Local pipe conditions will include scale accumulation and indeterminant pipe size and geometry.

The environment will subject the flowmeter to various forms of mechanical and chemical distress. In addition to the forces associated with fluid contact, the impingement of particles

entrained in the gas is expected. Certain components of the natural gas mixture cause corrosion in some materials making chemical stability a consideration. Furthermore, scale and other contaminants accumulate on intrusions into the gas stream and settle along the bottom of the line. While none of these forms of attack is particularly severe individually, the combination calls for a robust device which will provide reliable operation over a number of years under a variety of conditions.

2.2 Functional Requirements

The stated intent of the device under study is to provide a measurement of flows between districts in Consolidated Edison's distribution system. The points at which the measurements must be made are located throughout New York city and may be reached only via excavation. It is estimated that the cost of a typical orifice metering station would be several hundred thousand dollars. The cost of an Annubar metering station is about two thousand dollars [7]. The disparity between these costs arises from the requirements for major excavation, long straight runs of pipe, and interuption to service associated with the installation of an orifice metering station. The difference in cost between these flowmetering devices may be eliminated for the proposed ultrasonic flowmeter by imposing the following constraints.

First, service cannot be interrupted for either installation or calibration of the flowmeter. This means that the device must be installed in a live main. This is most commonly accomplished by welding a flange containing an airlock onto the main. A hole is drilled in the wall of the main with a bit that rotates in the airlock. The flowmeter is then inserted through this hole. It is important to note that flow cannot be stopped even momentarily for calibration at a zero flow point.

Second, excavation is to be minimized by requiring access to the upper portion of the

line only. While access to the top of the line may be easily achieved, access to the sides and bottom of the line would be significantly more difficult and could pose a threat to the structural integrity of the line.

Finally, the device would be subjected to rough handling throughout the installation process. For instance, backfilling of the excavation at an installed meter could damage external fittings. As a consequences of the limited installation accuracy achieveable in the field, it is very likely that a certain degree of misallignment would exist. Thus the device must operate accurately even though its position will be somewhat indeterminant.

2.3 Accuracy Requirements

As a consequence of rapidly rising energy costs, concern over the large quantity of unaccounted for gas lost through theft or leakage has grown considerably in recent years. An effort has been made to ascertain various characteristics of the performance of the distribution system to increase its effectiveness and reliability. Toward this end interdistrict gas flows are monitored. The measurements of these flows are used for internal purposes to the company and not for custody transfer. Thus there are no regulatory requirements for a specific accuracy level.

The accuracy required of the flowmeter developed for this thesis is best expressed in terms of the smallest quantity of gas of concern rather than as percentages of measured flowrates. What this implies is that the accuracy of velocity measurement expressed as a percentage of the measured quantity becomes less important at low velocities. The specification of the accuracy for the device under study is presented in terms of minimum resolveable flow (MRF). This expression refers to the smallest increment of flowrate that can be determined by the device. This concept is illustrated in Figure 2-1.

The curve represents flow over a typical day. The area under the curve is the total

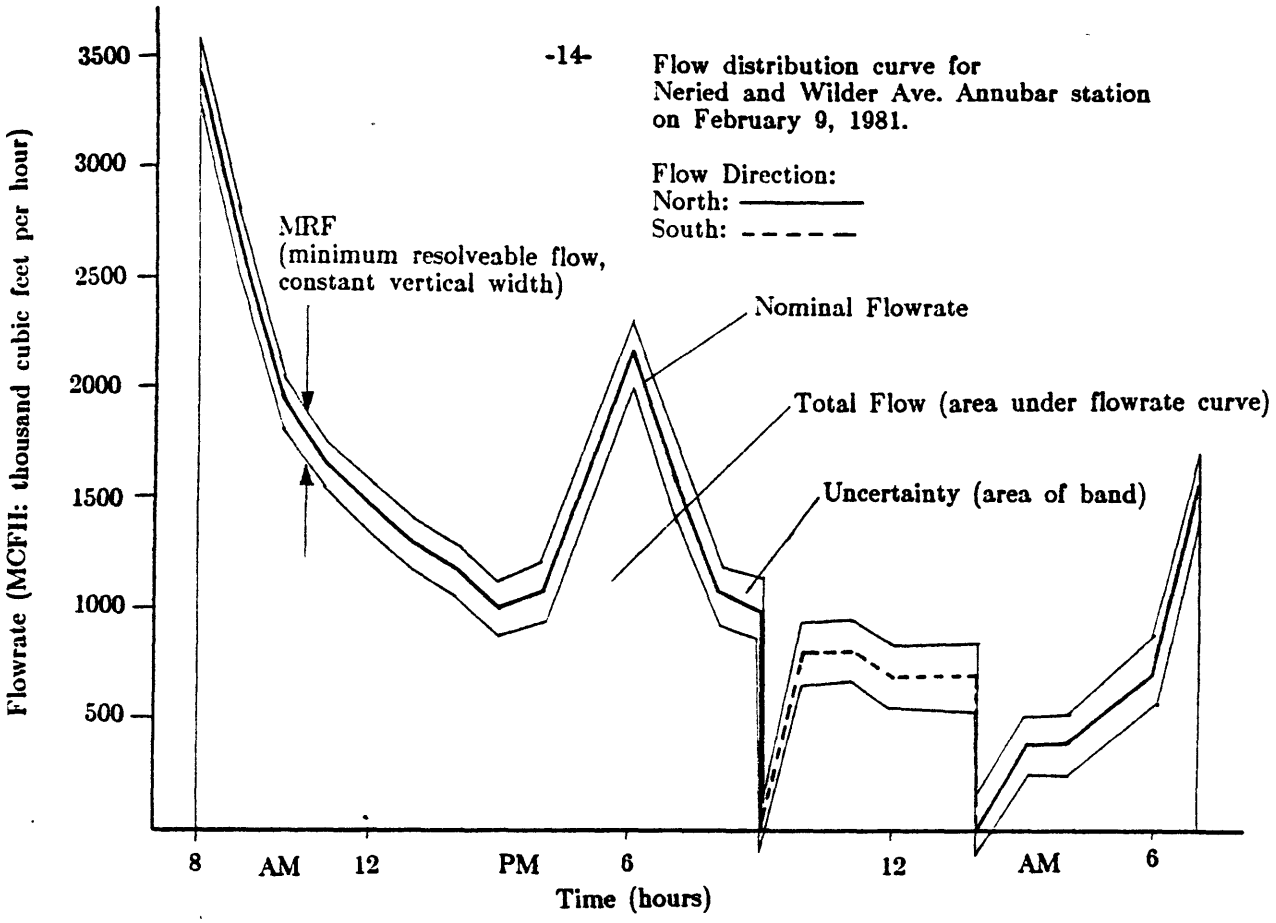

Figure 2-1: Minimum Resolveable Flow

quantity of gas transfered that day. The vertical width of the band is the MRF. Note that this is shown as a constant value. The uncertainty of the total quantity is represented by the area of the band. The accuracy of the measurement in percentage terms is obtained by dividing the MRF by the flowrate. Note that this percentage is high for low flows. It is clear from the figure that accuracy is best enhanced by uniformly decreasing the MRF. Attempts to produce very high accuracy relative to very low flows will be costly and not very productive.

It is desired that the total flow be measured to an accuracy of $\pm$ 0.5 per cent [8]. This corresponds to a MRF equal to 1 per cent of the average flowrate. Consolidated Edison provided monthly flow figures covering a period from October 1980 to September 1981 for the Nereid and Wilder Ave station. The total of the absolute value of flow in both directions averaged 752,896 MCF per month over this period. The unit MCF represents 1000 cubic feet of natural gas at standard temperature and pressure. This corresponds to an

average flowrate of 1031.25 MCFH over this period. The unit MCFH represents a flowrate of 1 MCF per hour. The desired minimum resoveable flow is 10.31 MCFH.

Chapter 3

The Ultrasonic Flowmeter

A number of techniques involving the propagation of acoustic signals have been used to measure fluid flow. Previous work on the measurement of gas flow has been performed using shock pulses and tone bursts travelling along direct trajectories [14]. The use of direct trajectories requires that transducers be installed on opposite sides of the gas line. Furthermore, calibration generally must be performed under no flow conditions. The requirements of the application discussed herein preclude the use of these existing techniques. This section contains a discussion of the underlying principles and practicle realization of a device using reflected and direct components of sonic pulses to determine flowrate. Generation of a shock pulse and information handling are covered. The synthesis of an experimental model is described. A discussion of alternative ultrasonic methods is included in Appendix B.

3.1 Principles of Operation

As a sound wave travels through moving media, the wave has a total velocity of the sonic velocity, c, of the wave plus the velocity of the media. Thus waves travelling in a downstream direction will travel faster than c while waves travelling upstream will be slower. The configuration where direct pulses propagate in a plane passing through the centerline of the pipe is shown in Figure 3-1.For counterpropagating waves travelling along a trajectory that is located in this plane and inclined with respect to the flow direction, the following relationship is valid [17].

$$V = \frac{L^2+D^2}{2L}\{1/t_d - 1/t_u\} \tag{3.1}$$

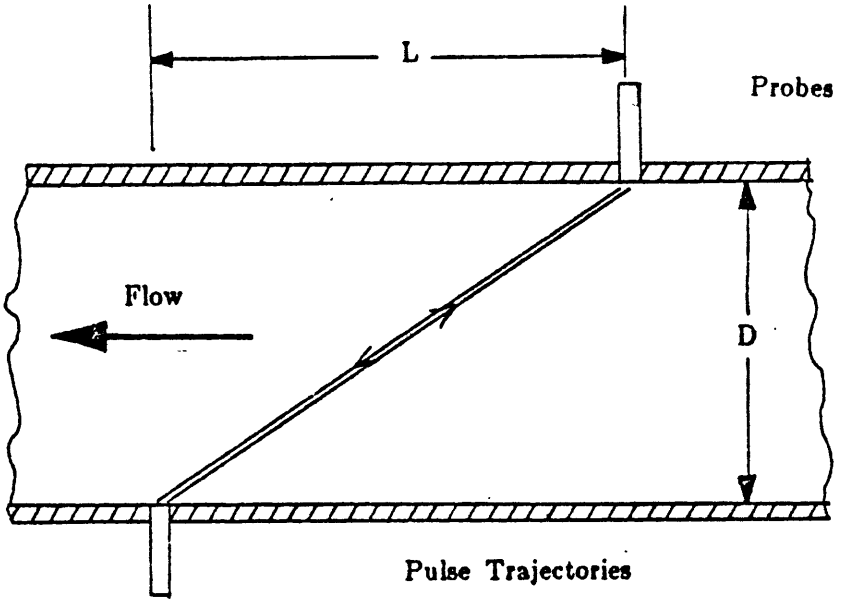

Figure 3-1: Basic Configuration Used in Existing Flowmeters

where:

- L = axial separation of the probes.
- D = diameter of the pipe.
- t_u = upstream flight time.
- t_d = downstream flight time.

The velocity described by this equation is the average velocity of flow in the plane of the signal trajectory. For flows at low Mach numbers it can be proved that deviations of the signal trajectory from a straight line will not effect information derived from the signals. Furthermore, it can be shown that the relationship remains valid for the limiting cases in which the pulse is treated as a plane wave or a uniform spherical wave [9].

As the nature of the application requires that access to the gas line be limited to its upper section, it was decided to locate both sending and receiving transducers near the top of

the line and use a trajectory reflecting off of a diametrically opposed surface. This geometry is shown in Figure 3-2.

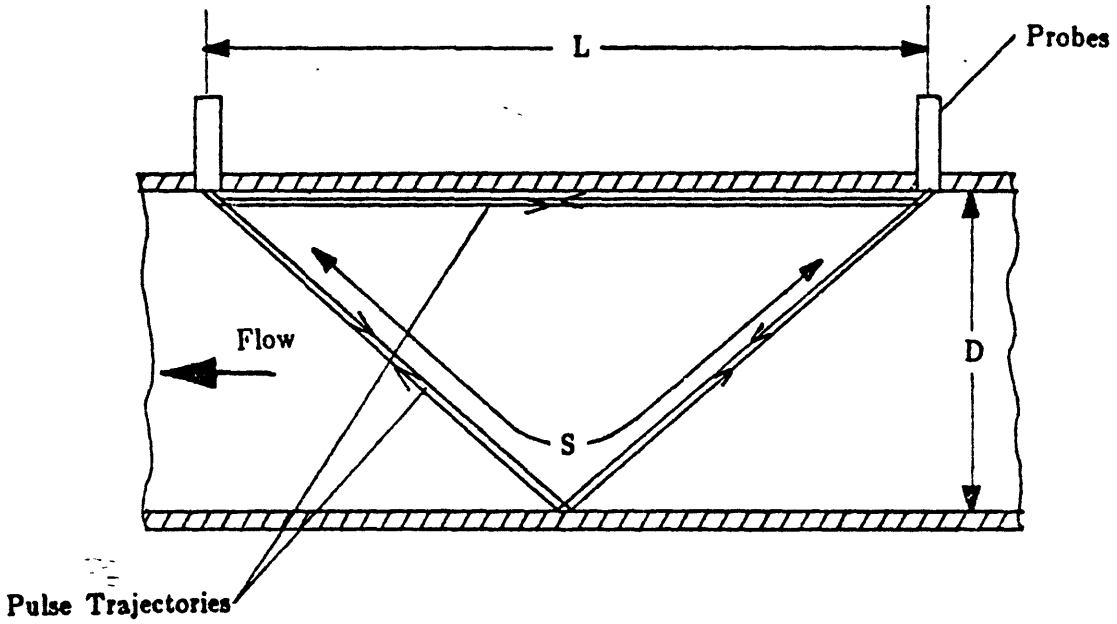

Figure 3-2: Proposed Flowmeter Using Reflecting Configuration

The equations used to describe the direct pulse are applicable to the reflected signal for two extremes of pulse modeling. The first model is a collimated beam reflecting off of a region which is essentially flat in comparison to the diameter of the beam. The second is of a uniform spherical pulse reflecting off of the inner surface of a cylinder. The earliest received component of the reflected spherical pulse will follow the trajectory of the collimated beam model. This path necessarilly lies in the plane passing through the centerline of the pipe. The equation relating flight times to line averaged velocity is then:

$$V = \frac{S^2}{2L}\{1/t_d - 1/t_u\} \tag{3.2}$$

where S is the total reflected path length.

Note that as flow reversals occur, the difference between the reciprocals of the flight

times and the velocity will change sign. The unit performs equally well for flow in either direction.

The highest flowrate that can be determined accurately using the linear equations is limited only by Mach effects. As the flowrate approaches the sonic velocity, the pulse trajectories deviate from straight lines. These deviations introduce non-linearities into the derivations on which Equations (3.1) and (3.2) are based. The non-linearities will result in errors on the order of one per cent in these equations when flow velocity exceeds 20 per cent of the sonic velocity. The practical upper limit of the useful flow measurement range is 20 per cent of the sonic velocity or 260 feet per second: ie., much higher than the anticipated 30 feet per second.

For highly turbulent flow (Reynolds number $>$ 10,000) the average velocity in the plane of the centerline is related to the average velocity of the entire cross-section by the well known logarithmic relationship [16]:

$$m = 1.119 - .011\log(Re) \tag{3.3}$$

where:

- Re = Reynolds number

The quantity m is the ratio of the average velocity in the plane passing through the pipe centerline to the average velocity over the cross-section. It is used as a profile correction factor in the calculation of flow. For typical flows in a two foot diameter main. the Reynolds number will be on the order of 10^6.

Equation (3.3) provides a correction factor that is applicable for fully developed turbulent flow in a cylindrical pipe. Deviation of flow behavior from this model will affect the relationship between measured and actual flowrates. It is possible to derive an appropriate correction factor for any flow profile provided that an analytical description of the profile is available.

3.1.1 Automatic Calibration

An important consequence of the reflected signal concept is that it allows self calibration of the device without stopping the flow. The straight line separation of the probes and the path length must be determined. This may be accomplished in the following way.

The sonic pulse will propagate spherically, but the strength of the wave may be collimated to some degree. It is possible to detect and discriminate between the reflected and direct components of a pulse shown in Figure 3-2. Furthermore, it is possible to determine the average flight times of the pulse components in addition to their differences. The average flight time is the same as the flight time under no flow conditions and will be constant regardless of flow velocity. The path lengths may be calculated using the averaged flight times and the speed of sound. The probe separation distance (L) and the reflected trajectory length (S) are given by:

$$L = \frac{t_{dl}+t_{ul}}{2} c \tag{3.4}$$

and

$$S = \frac{t_d+t_u}{2} c \tag{3.5}$$

where:

- t_{dl} = downstream flight time along L path
- t_{ul} = upstream flight time along L path

The values t_d and t_u are the S path flight times used in equation (3.2). The sonic velocity is determined through temperature measurement and chromatographic analysis of the gas composition.

3.1.2 Flowrate Calculation

The flowmeter, having determined the line averaged velocity, uses additional information to get the flowrate in standard volumetric form. This quantity is given by:

$$Q = mVA\{\rho_a/\rho_s\}F_{pv}^2 \tag{3.6}$$

where:

- Q = volumetric flowrate at standard conditions
- m = profile correction factor from Equation (3.3)
- A = cross-sectional area of pipe
- ρ_a = actual density
- ρ_s = standard density
- F_{pv} = supercompressibility factor

Equation (3.6) is iterative in that Re must be known to calculate m. However, m varies only slightly with Re thus, for periodic, continuous flow measurements, an approximation of m based on the most recent flow measurement (i.e., one iteration) is sufficient. The standard density is constant. The values of ρ_a and F_{pv} are required for most common gas flow measurement methods and may be obtained by accepted conventional means. The area of the pipe may be calculated directly from the calibration information using:

$$A = \pi\{S^2-L^2\}/16 \tag{3.7}$$

A consequence of this calibration technique is that the pipe diameter is measured periodically. Thus, changes in pipe size or probe movement caused by thermal contraction and expansion will not affect the accuracy of the flow measurement.

The trajectories of the pulses lie in the plane that coincides with the centerline of the pipe. Concentric swirl produces velocity components which are perpendicular to that plane, thereby leaving the transit time difference unaffected. The effects of asymetry or other poor

flow conditions are impossible to analyze meaningfully in that analytical descriptions of various types of non-uniform flow conditions generally fail to represent actual flow behavior.

3.1.3 Accuracy Analysis

The accuracy of the ultrasonic flowmeter is determined primarily by its minimun resolveable flow. Variations in other parameters of flow measurement and the non-ideal behavior of actual hardware also affect overall accuracy. These effects are discussed below. The MRF of the flowmeter depends on the smallest increment of flight time that can be detected. The MRF, in terms of velocity rather than volumetric flow, and time increment are related by:

$$\delta V = \{c^2/2L\}\delta t \tag{3.8}$$

where:

- δV = minimum resolveable velocity
- δt = smallest measureable time increment [12]

For the application under consideration, the desired MRF is 10.31 MCFH in terms of volumetric flowrate at standard conditions. For a line pressure of 160 psig the corresponding MRF is about 0.867 MCFH. In a two foot diameter line the minimum resolveable velocity will be 0.077 ft/sec. The sonic velocity is about 1300 ft/sec and typical probe separation distance will be 4 feet. Thus the necessary time increment is given by Equation (3.8) as 3.6×10^{-7} seconds. In fact, flight times on the order of those used by this flowmeter can be measured to a resolution of 1.0×10^{-7} seconds with off-the-shelf components. Should greater accuracy be desired, it is possible to achieve a resolveable time increment that is shorter than the rise time of the pulse. The use of consistant pulses and detection equipment permits triggering of the timing hardware at a specific, repeatable point on the leading edge. Since the MRF may be made considerably smaller than necessary for adequate performance, the accuracy of the device will be limited by other factors.

3.1.3.1 Flow Measurement Error

Uncertainty in flow measurement will result from uncertainty of the parameters in Equation (3.6). Knowledge of the profile correction factor is well established and sufficiently precise so that it will not contribute significantly to overall error for a standard profile. The values of ρ_s and F_{pv} are required for every accepted method of natural gas flow measurement and may be determined sufficiently accurately by existing techniques. The value of ρ_s is an empirical constant which is known with a very high accuracy. The value of A depends on the calibration information and the geometry of the pipe. Since the transit times are measured to high accuracy, the souce of error in the area term will be dependent on uncertainties of the pipe geometry. Such uncertainties arise from out of roundness and scale accumulation. It is not possible to eliminate this source of error without direct inspection of the inner surface of the pipe. It is significant to note that any method using point or line velocity measurement to infer volumetric flowrate will be subject to this uncertainty. Other errors in flow measurement arise from the uncertainty with which V is determined.

3.1.3.2 Velocity Measurement Error

It has been established that the minimum resolveable velocity of the ultrasonic flowmeter is sufficient to provide good performance. However, the practical implementation of the device introduces a number of sources of error. These uncertainties have to do with the relationship between the centerline average velocity and the time-of-flight measurements. The following factors are known to contribute error.

1. Constant turbulent flow has local random velocity variations about an average. The ultrasonic flowmeter detects instantaneous velocity. Therefore a number of samples must be taken to come up with a value that converges about the true average velocity.

2. Fixed time delays can exist in the timing equipment. It is necessary to adjust the flowmeter so that these delays are equivalent for upstream and downstream pulses. This causes errors in the flow equation to cancel out [23]. The delays can be balanced but not eliminated; thus, they would still introduce errors in the path

length equations. The delays tend to be small relative to the transit times and this error would be negligible.

3. The transducers have a finite size and will not be perpendicular to both direct and reflected pulse trajectories. Thus the measured path length could vary as a result of detection of the pulses by different regions of the transducer. In addition, a pulse striking a transducer at an oblique angle will cause the detected leading edge to have a longer rise time than that of a pulse with a normal incident angle. These effects must be minimized through adjustment prior to installation and careful transducer design [5].

4. The probes on which the transducers are mounted can cause local disturbances in the flow which affect pulse flight times. This can be minimized but not eliminated through careful probe design [9].

5. It is possible that the axis of probe separation (the straight line between the probes) may be misaligned with respect to the plane coinciding with the centerline of the pipe. For swirl free flow, a misalignment of 1 inch over a probe separation of 4 feet introduces an error of 0.02 per cent. The presence of large amounts of swirl (45 degree swirl angle) would introduce an error on the order of 1.0 per cent. Careful alignment of the unit is necessary to eliminate the effects of severe swirl.

6. Scale may accumulate on the transducers and cause path length drift. This ultrasonic flowmeter measures path lengths directly and eliminates drift error. The accumulations can degrade transducer performance [19].

7. Accumulations of scale and other deposits may be particularly severe along the bottom of the line. It is possible to prevent these deposits from interfering with the reflection of the pulse by locating the transducers away from the exact top of the line. Thus, the reflection region would be shifted away from the bottom of the line.

Experience with other types of ultrasonic flowmeters shows that it is possible to minimize the effect of these sources of error through careful design.

3.2 Behavior and Generation of Shock Pulses

The operation of this type of ultrasonic flowmeter requires the use of a pressure pulse with a rise time on the order of one microsecond. A pulse with the rise time and strength required occurs in gases as a shock wave. Thus weak shock waves must be generated periodically. This may be accomplished through a number of established techniques. The nature of shock waves and three methods of generating them are discussed.

3.2.1 Weak Shock Phenomena

A shock wave is a travelling discontinuity of pressure and density. Its speed exceeds the speed of sound. The velocity of a shock is related to its strength by:

$$P = \frac{2k}{k+1}\{M^2-1\} \tag{3.9}$$

where:

- P = Ratio of the shock pressure rise to the local static pressure.
- k = Ratio of specific heats.
- M = Ratio of the shock velocity to the sonic velocity [21].

For weak shocks, the Mach number, M, approaches 1 and the shock velocity approaches the sonic velocity. It is desireable to use weak shocks so that the difference between shock velocity and sonic velocity is negligible.

A shock arises from a steep pressure pulse. Since sonic velocity increases with temperature and temperature increases with pressure, the trailing edge of a compression pulse will have a tendancy to overtake the leading edge. Since the trailing edge can never pass the leading edge, a discontinuity results. The thickness of a shock wave is defined by non-isentropic molecular interactions and is on the order of 10^{-5} inches [24]. It has been demonstrated that, for a natural gas application, a pressure pulse of less than 100 microseconds is necessary and sufficient to form a shock with a rise time of 0.1 microseconds. A shock tube of adequate length to permit the steepening phenomena to take place must be used. The rate at which the steepening phenomena occurs depends on the nature of the gas and the shape of the initial pulse. The length required to permit steepening cannot be predicted accurately. In practice, shock development lengths of 1 to 3 feet have proven adequate [9].

It is significant to note one other property of shock steepening phenomena. The leading

edge of the pulse will be blurred somewhat by reflection off of a surface that is not completely smooth. The steepening phenomena regenerates the sharp leading edge after such a reflection. Thus, the flowmeter will not be affected by minor deposit accumulations on the inner surface of the pipe.

The minimum acceptable strength of the shock wave is determined by the sensitivity of the detecting transducers and the attenuation of the wave as it propagates and reflects. The maximum acceptable strength is limited by deviation of the shock velocity from the sonic velocity. The need for a shock such that P does not exceed 0.03 is shown in the following two sections. The Mach effects are shown to be acceptable.

3.2.1.1 Signal Detection

Transducers capable of picking up acoustic pulses are commonly available for wide ranges of frequency and sensitivity. The scheme used in the design of this prototype was to have the incoming signal excite a piezoelectric crystal at its resonant frequency of 5 MHz. The mechanical Q of the crystal was over 500. Thus fast transients of large amplitude with minimal intrinsic delay are easily achieved [18].

The necessary shock strength is determined by the desired signal to noise ratio at the detector. The nature of the flowmeter configuration calls for the observation of two pulse components sequentially. It is desireable to make the second pulse received (S path) somewhat stronger than the first. Furthermore, only fast transients are of concern. Therefore mechanical noise below say 100 kHz may be electrically filtered out. Since mechanical noise in the vicinity of 1 MHz seldom occurs in nature (or New York) over 110 db, an L path pulse with strength of 120 db at the receiving crystal is sufficient.

3.2.1.2 Shock Attenuation

It can be shown that for a uniform spherical pulse, the L signal would be stronger than the S signal. However, the shock may be collimated along the S path, attenuating the L path. Thus the strength of the received S signal will determine the necessary initial signal strength. It is practical to have the the amplitude of the S pulse exceed that of the L pulse by a factor of 2 (6dB) at the receiver.

In the absence of losses, the energy of a spherical wave is constant. Thus:

$$p_1 R_1 = p_2 R_2 = \text{constant} \tag{3.10}$$

where p is the shock pressure rise and R is the distance from a point source [11]. For probe separation of 4 feet in a 2 foot diameter line, $R_2 = S = 5.66$ feet.

The actual source will have a finite size of say .5 inches in diameter. It is conservative to treat this real area as being a distance equal to its radius from a virtual, infinitesimal point source. Thus $R_1 = 0.021$ feet. It follows that p_1 exceeds p_2 by a factor of 269 or about 49 dB.

Experiments with electromechanical pulse generators similar to the ones descibed below indicated that transmission will not be loss free. Attenuation was found to be less than 10 dB [9]. Also, there will be losses in the reflection. These losses will tend to be small, even for somewhat rough surfaces, as a consequence of the poor acoustic coupling between a metal and a gas. It is reasonable to estimate reflection losses at less than 5 dB [11].

Adding the rather conservative loss figures to the necessary strength of the received signal gives an initial signal strength of about 190 dB or 5 psi for a shock delivered via a 0.5 inch tube. This corresponds to a ratio of the pressure rise of the shock to the absolute pressure of 1.029 at a static pressure of 160 psig.

3.2.1.3 Mach Effects

It has been shown that the pulse velocity does not affect the flow equations (3.1) and (3.2) directly [9]. However, the configuration of the flowmeter under study requires that the path lengths L and S be calculated using transit time information. These values will be affected by Mach phenomena.

The Mach factor changes over the trajectory of the pulse. The average value of the Mach factor over an arbitrary path is given by:

$$M_{ave} = \{1/X\}\int_{x_1}^{x_2} M\, dx \tag{3.11}$$

where:

- M_{ave} = Average Mach factor.
- X = Length of trajectory between points x_1 and x_2.

Let us consider the case where:

$$X = L - R_1 \tag{3.12}$$

Equations (3.9) and (3.10) may be combined with Equation (3.11). For a value of k = 1.4, integrating over the L path gives [20]:

$$M_{ave} = \frac{1}{L-R_1}\left[\sqrt{x(K+x)} + [K/2]\ln\frac{K+x+\sqrt{x(K+x)}}{K+x-\sqrt{x(K+x)}}\right]_{R_1}^{L} \tag{3.13}$$

where:

$$K = \frac{P_1 R_1}{1.667} \tag{3.14}$$

Substituting the values of R_1 and L given above, P = 0.03 gives M_{ave} = 1.0030.

The preceding derivation is based on the assumption of lossless shock propagation. Since losses are known to occur, the value of M_{ave} given above overestimates the actual average Mach factor.

The results indicate that path length measurements will be distorted by a Mach related

error of less than 0.3 per cent. This error may be ignored or a correction factor based on the characteristics of actual hardware may be employed.

3.2.2 Rapid Opening Valves

Practical devices capable of generating a sufficiently steep pressure pulse would be fast opening valves. Two types are shown in Figures 3-3 and 3-4.

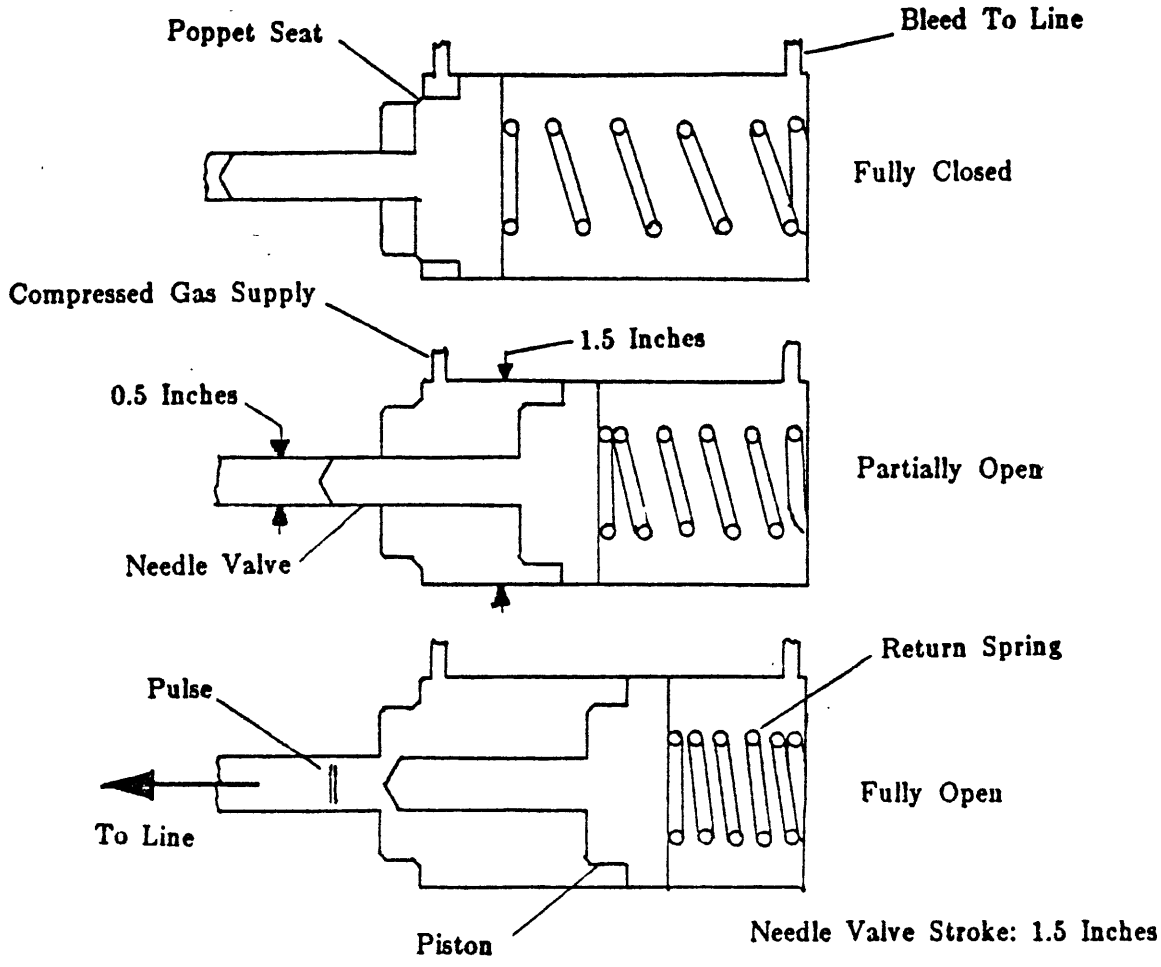

Figure 3-3: Rapid Opening Mechanical Valve for Generating Shock Pulses

For these devices, a pressure difference would be provided by an external compressor using gas drawn from the line as a working fluid. The valves would be opened rapidly enough to

provide the required pressure pulse and closed quickly enough to avoid the need for a large compressor.

The first type (Figure 3-3) is a purely mechanical valve. It is shown in three phases of its operation. Initially, the valve is closed and pressure is supplied to the plenum by an external compressor. When the pressure reaches a desired level, the poppet seat opens admitting elevated pressure to the chamber. The sudden large force accelerates the core and opens the valve sufficiently rapidly to generate a compression pulse.. The assembly is returned to a closed state by a spring. The compressed gas is vented into the line. For a valve of the dimensions shown, having a stroke of 1.5 inches and a core mass of .05 lb, a compressor providing 40 psi at a relatively low flow rate would be adequate.

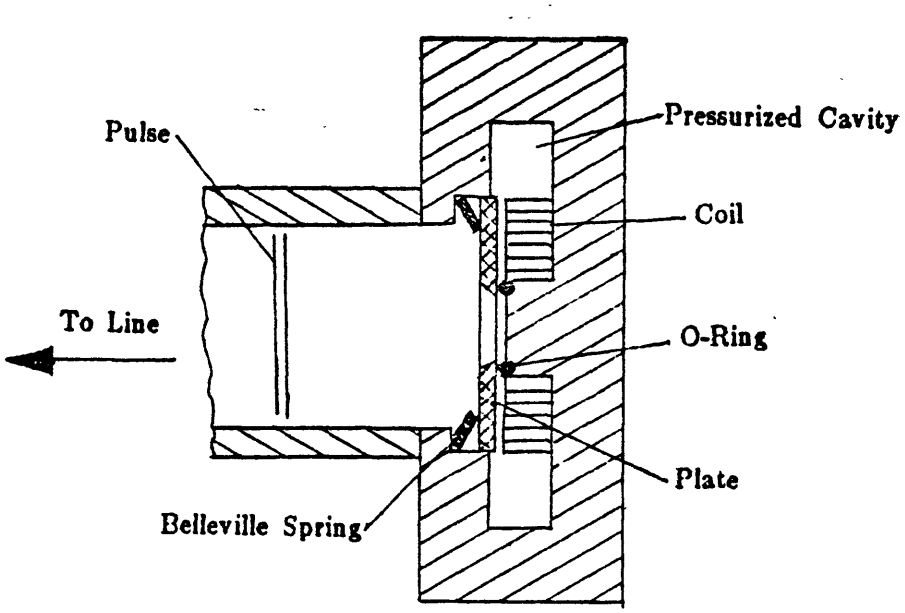

Figure 3-4: Rapid Opening Electromechanical Valve For Generating Shock Pulses

The second configuration (Figure 3-4) is based on a design which was developed for rapid injection of small amounts of fuel into a fusion research reactor [1]. The principal

components of this device are a spirally wound coil of ribbon wire and an aluminum plate. A capacitor is discharged through the coil setting up a locally strong magnetic field and corresponding eddy currents in the aluminum plate. A strong repulsive field occurs forcing the plate away from the coil. A small amount of gas is admitted in the form of a pulse. The valve closes from the elastic force of Belleville springs. Pulse durations of 60 microseconds have been achieved. The pressure difference between the line and the externally compressed gas would be lower than that required for the purely mechanical valve because the compressed gas would not be used to drive the piston. A pressure equal to the desired shock strength of 5 psi would be adequate. The mechanical forces in the seats and the Belleville springs are low enough to permit long life.

3.2.3 Eddy Current Piston

Another method of pulse generation would involve components similar to those of the electromechanical valve, above. In this device the pulse would be provided by the aluminum plate directly as shown in Figure 3-5.

A mechanism of this type has been used to generate shocks in liquids [15]. The driving forces between the coil and the plate would be much larger than those in the electromechanical valve. Two plates would be used to balance forces on the coil. No external compression of gas would be required. The piston would be accelerated to the sonic velocity of the fluid. Much of the energy of the piston would be dissapated through impact with the restoring springs. Thus, mechanical forces in the restoring springs would be large and fatigue could be a problem.

It should be noted that no commercially available devices employing the above mentioned techniques are manufactured for the specific purpose of generating shock pulses. However, each of the methods discussed utilizes existing technology and hardware.

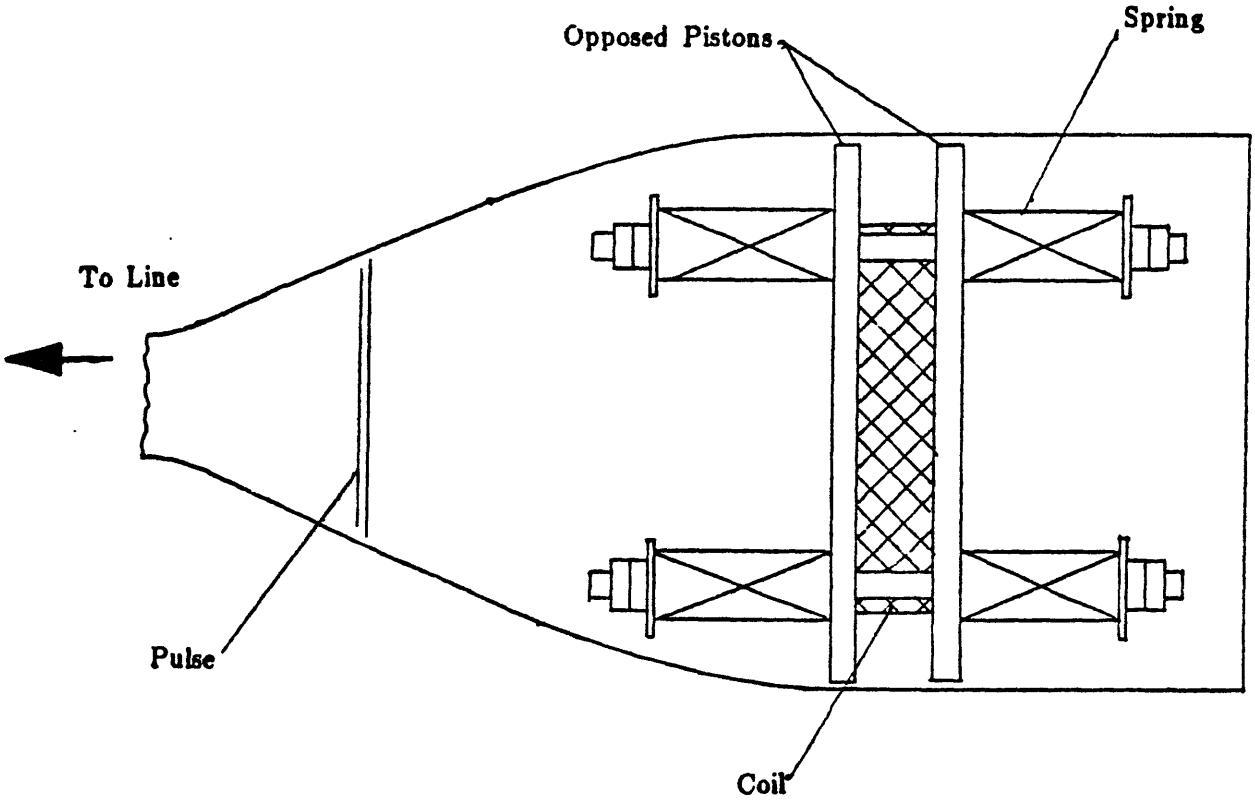

Figure 3-5: Eddy Current Piston for Gennerating Shock Pulses

3.3 Signal and Data Processing

A dedicated data acquisition and analysis system is required to transmit and detect the shock pulses and convert this information into a measurement of flow in near real time. The information handling system must perform a variety of tasks including:

- coordination of the pulse firing sequence.
- measurement of transit times.
- conversion of pressure, temperature, and density information into flow correction factors.
- calculation of flow rate and calibration information.

Fortunately, digital electronics are widely available in easy to use, reliable modular packages. An overview of a dedicated data processing system is shown in Figure 3-6.

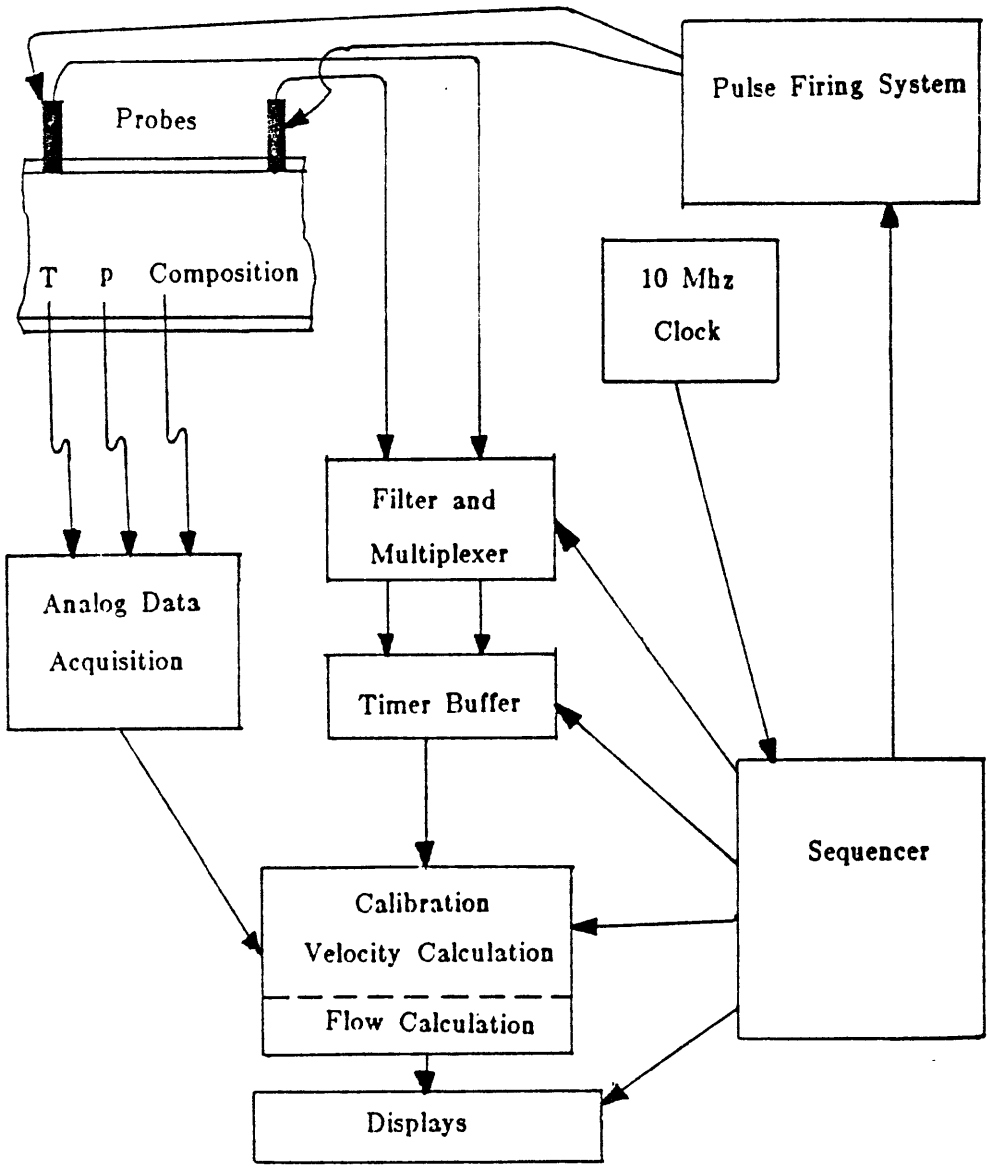

Figure 3-6: Control and Information Processing System for Ultrasonic Flowmeter

The system would be driven by a 10 MHz clock. All sequencing and timing measurements would use the clock output or multiples of it. A time increment of 10^{-7} seconds would be used. Integrating flowrate over a specified interval of time would give the total flow over the interval. A typical cycle would run something like this:

1. Obtain transit time information for one direction.

a. Shock generator sends pulses at regular intervals.

b. Detect and measure direct and reflected transit times for each pulse.

c. Store transit times in a buffer updating statistical information after each pulse.

d. Reject all information further than 3σ from the mean of the pulse flight times for each trajectory thereby reducing the effect of spurious signals.

2. Obtain information for other direction.

3. Update calibration data.

4. Calculate flow parameters based temperature, density, and static pressure.

5. Calculate velocity.

6. Calculate flowrate.

7. Calculate Reynolds number for next cycle.

8. Update total flow counter.

9. Repeat cycle.

3.4 Development of an Experimental Model

The ultrasonic flowmeter outlined in the preceding sections requires a dedicated electronic support system and a mechanical or electromechanical shock generator capable of functioning in a high pressure natural gas environment. In the interest of demonstrating the viability of the overall concept with the available time and resources, a number of simplifications were made to the proposed system. The most noteworthy difference is that tests were performed using ambient pressure air in a 1 foot diameter pipe rather than 160 psig natural gas in a 2 foot diameter main. The ability of the prototype to measure flow rates in air would demonstrate the suitability of using reflected and direct pulses for flow measurement and self-calibration in actual service.

The development and construction of an appropriate electromechanical shock generator

was determined to be beyond the scope of this project. For this reason, a starter's pistol was used as a reliable, expedient shock generator.

A dedicated data reduction system would be too inflexible and too expensive for initial studies. A recording digital oscilloscope was able to measure the flight times accurately while providing useful information on the nature of the transmitted pulses. Other measurements were performed with analog instrumentation. Data reduction was performed by hand.

3.5 Prototype Design

A cross section of the prototype is shown in Figure 3-7. A detail of the probe tip is shown in 3-8. The units consisted of 1.5 inch diameter copper tube bodies housing the shock guides, crystals, and preamplifiers. The shock guides were 3/8 inch copper tubes with ends milled at 22.5 degrees, to which copper plates were soldered. The plates reflected the waves at a 45 degree angle to the pipe centerline through an opening in the side of the line. Shock guides were used as a chasis for the crystal supports and internal electronics. An aluminum cylinder was used to align the guide and crystal support with respect to the body. The guide was secured to the cap with hose clamps. All possible leak paths were sealed with teflon tape. A photograph of the prototype with the body removed is presented in Figure 3-9.

The transducers used were 3/8 inch diameter, 0.015 inch thick LTZ-5 lead-titanate piezoelectric crystals. They were supported by the leads which were soldered directly to their faces. The braided leads were twisted around a solid core for added rigidity. The lead assembly passed through a plastic tube which was suported by compliant foam. This was done to minimize the effects of mechanical noise from the test rig.

Preamplifiers shown in Figure 3-10 were built using Analog Devices AD521 instrumentation op amps. The AD521 is a high grade, low cost differential amplifier. The

Figure 3-7: Ultrasonic Flowmeter Prototype Cross Section

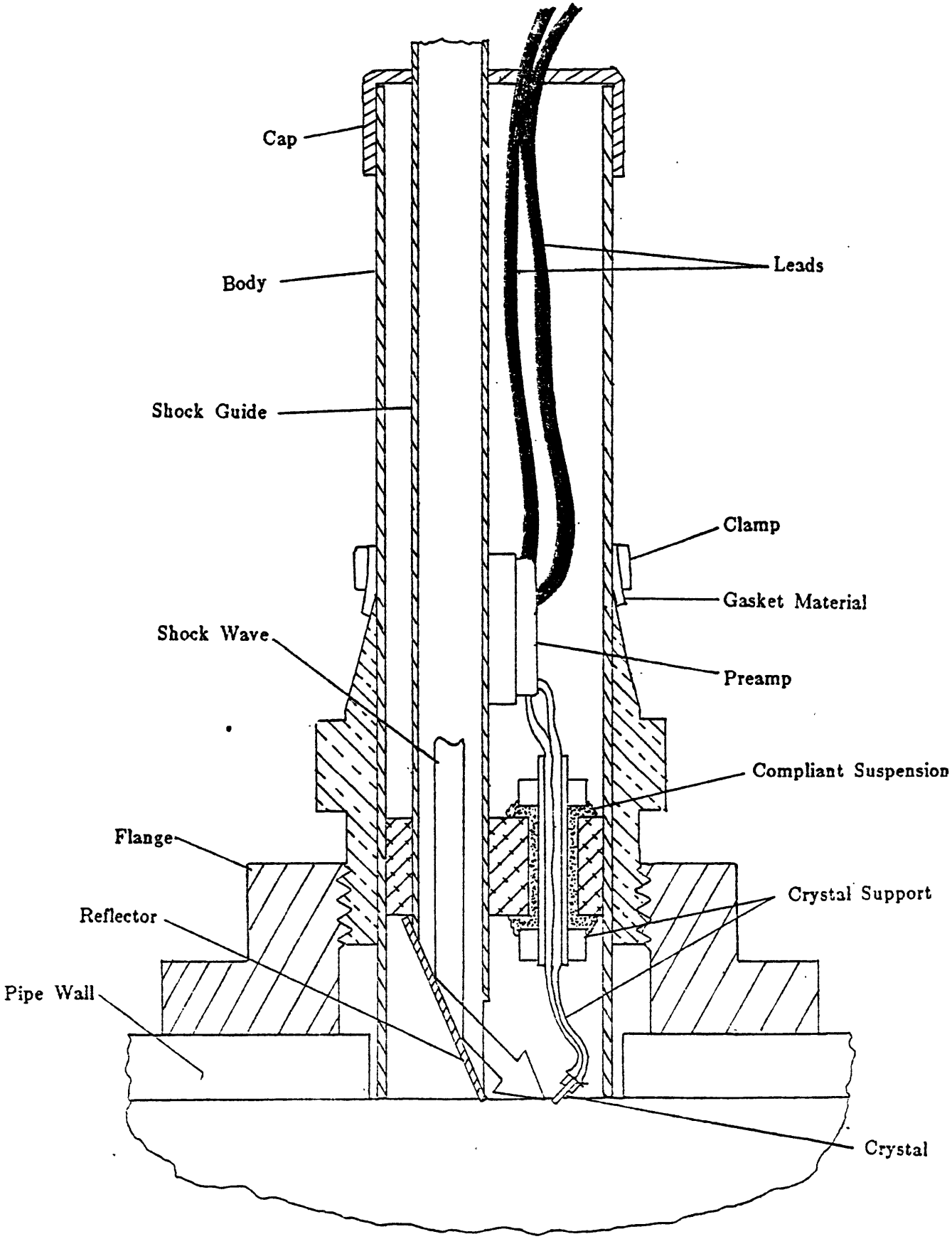

Figure 3-8: Detail of Probe Tip

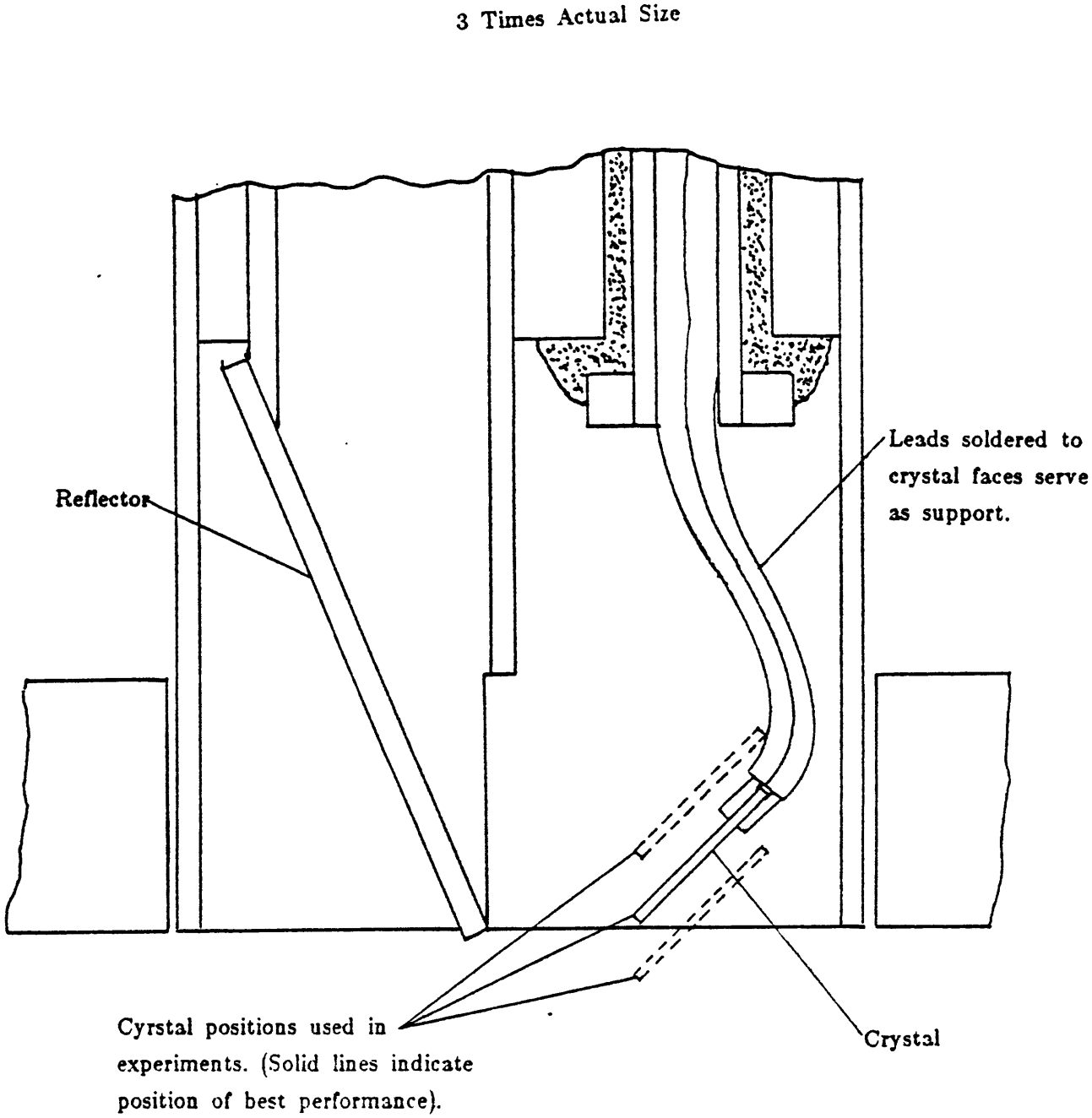

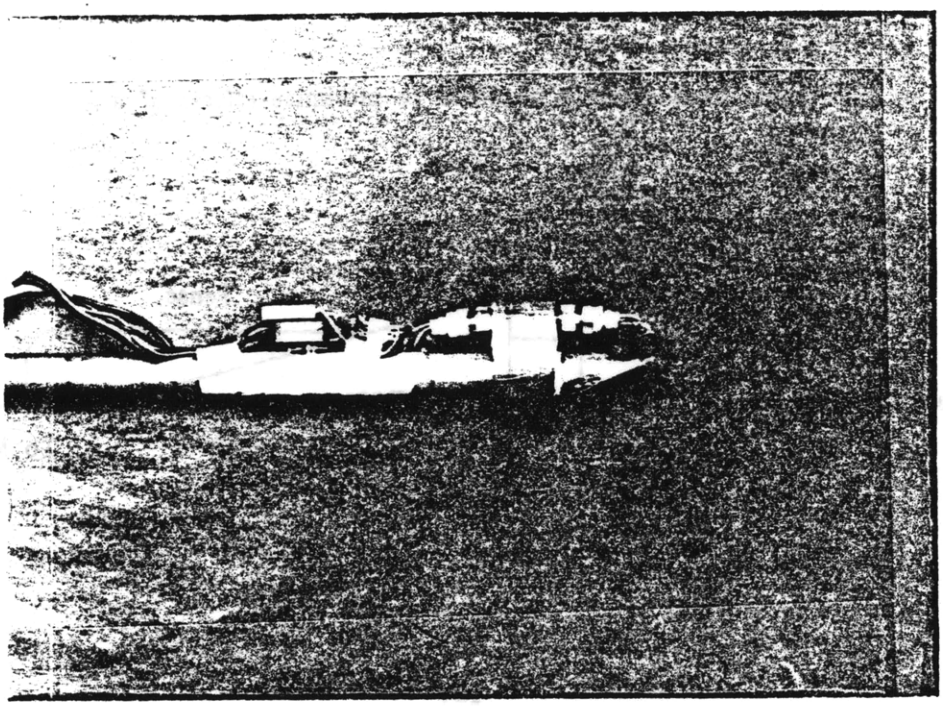

Figure 3-9: Prototype, Body Removed

preamps were initially built to provide gains of 1000 which were later reduced by a factor of 10 as a result of unexpectedly high signal strength. The preamps had adjustable offsets permitting matched DC levels. They were powered by an external supply consisting of two 15 volt batteries. The leads were coaxially shielded. This was done to prevent 60 Hz and rf noise from interfering with the signals.

The probes were connected to a digital oscilloscope via a multiplexer and high pass filter shown in Figure 3-11. The multiplexer permitted the use of a single timing circuit for both upstream and downstream trajectories. This was done to eliminate possible inconsistancies between dual timers.

A high pass filter, also shown in Figure 3-11, was used to eliminate mechanical noise. Since only fast transients with components on the order of 10^6 Hz are of interest, the filter was designed to cut frequencies below 10^5 Hz with a constant -20 dB attenuation below 10^4 Hz.

Signal from crystals amplified to minimize effects of noise.

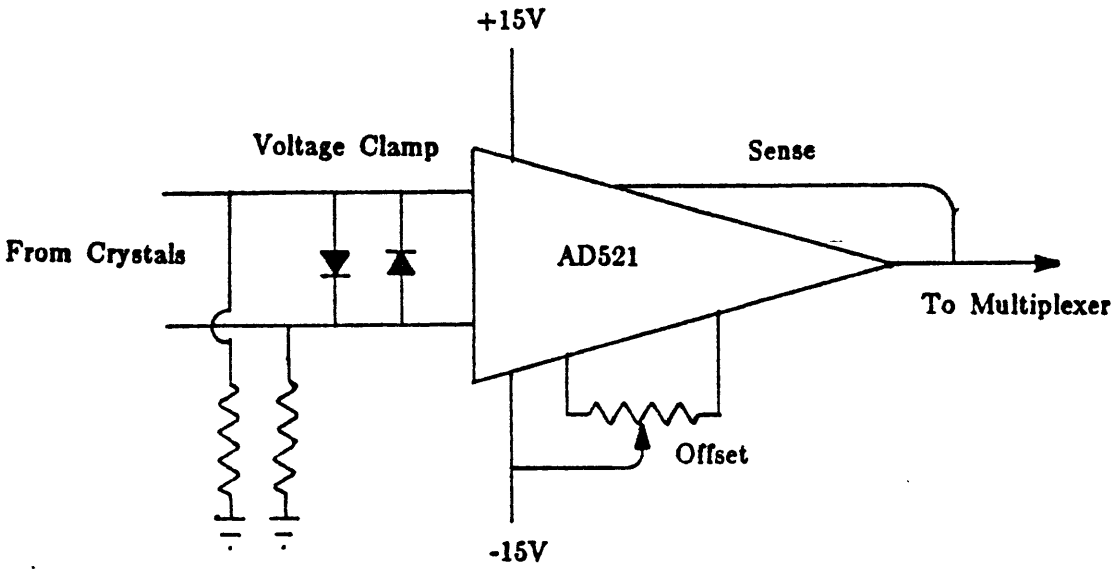

Figure 3-10: Schematic of Preamplifier Installed in Prototype

Interface between probes and data acquisition.

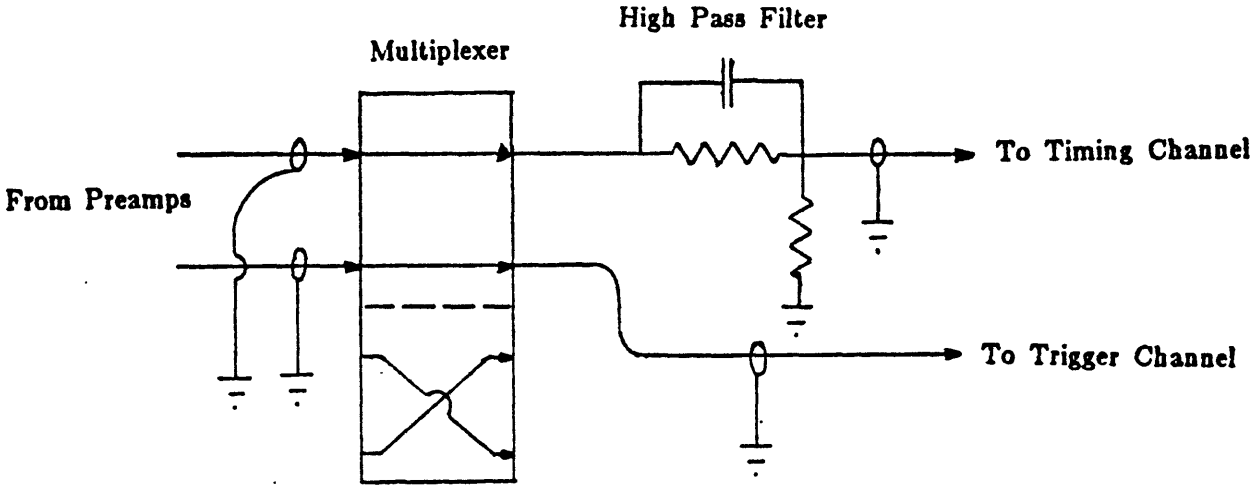

Figure 3-11: Multiplexer and High Pass Filter

Chapter 4

Experimental Methods and Hardware

A model of the proposed ultrasonic flowmeter was built and tested to demonstrate the viability of the concept and determine the outstanding problems that should be addressed in phase two. This section discusses the goals of the test program, the hardware and techniques employed, the accuracy of the instrumentation, and the accuracy of the methods used to obtain results.

4.1 Objectives of the Test Program

Experiments were designed to explore three major areas:

1. Establish suitability of the various components of the model.
    a. Ability of piezoelectric crystals to receive and transduce meaningful information.
    b. Adequacy of electronic support system.
    c. Adequacy of mechanical design (vibration isolation, etc.)
2. Demonstrate systemic performance characteristics of the prototype
    a. Accurate measurement of pulse flight times.
    b. Viability of reflected pulse detection.
    c. Viability of self-calibrating technique.
    d. Good reflective surface.
    e. Poor reflective surface.
3. Demonstrate ability of the prototype to measure flow rate.

4.2 Test Rig

A fifty foot long test facility was built in the basement of building 3. The rig, shown in Figure 4-1, consisted of a 45 foot long pipe with a one foot nominal inside diameter.

Flow was provided by a blower at the downstream end thus eliminating the effects of compressor pulses on the tests. The unit employed was a 5 hp Peerless PW14 capable of delivering 1300 cfm at 9 inches of water. Velocity was varied by venting air into the line between the orifice plate and the blower. This approach prevented excessive motor loading caused by restrictive flow control at low velocities. The instrumentation and installation of an Annubar flow sensor, also tested, are discussed in Appendix A.

For flow tests, the ultrasonic prototype was mounted with 14 diameters of straight pipe upstream preceded by a flow straightener. A downstream length of 4 diameters separated the test section from the flow straightener at the upstream end of the reference measurement section.

4.3 Reference Instrumentation

Reference flow measurements were performed using a sharp edged circular orifice plate with flange taps. An orifice diameter of 5.500 inches was used. Taps were located one inch from the orifice plate surface. The orifice plate was installed with an uninterupted straight upstream pipe length of 20 diameters and a downstream length of 5 diameters in accordance with ASME recommendations. The upstream section was preceded by a flow straightener composed of 2000 plastic straws.

Two water manometers were used in parallel to provide a wider useful differential pressure measurement range than could be achieved by one. A conventional U-tube manometer with a range up to 16 inches of water and a resolution of ± 0.05 inches of water

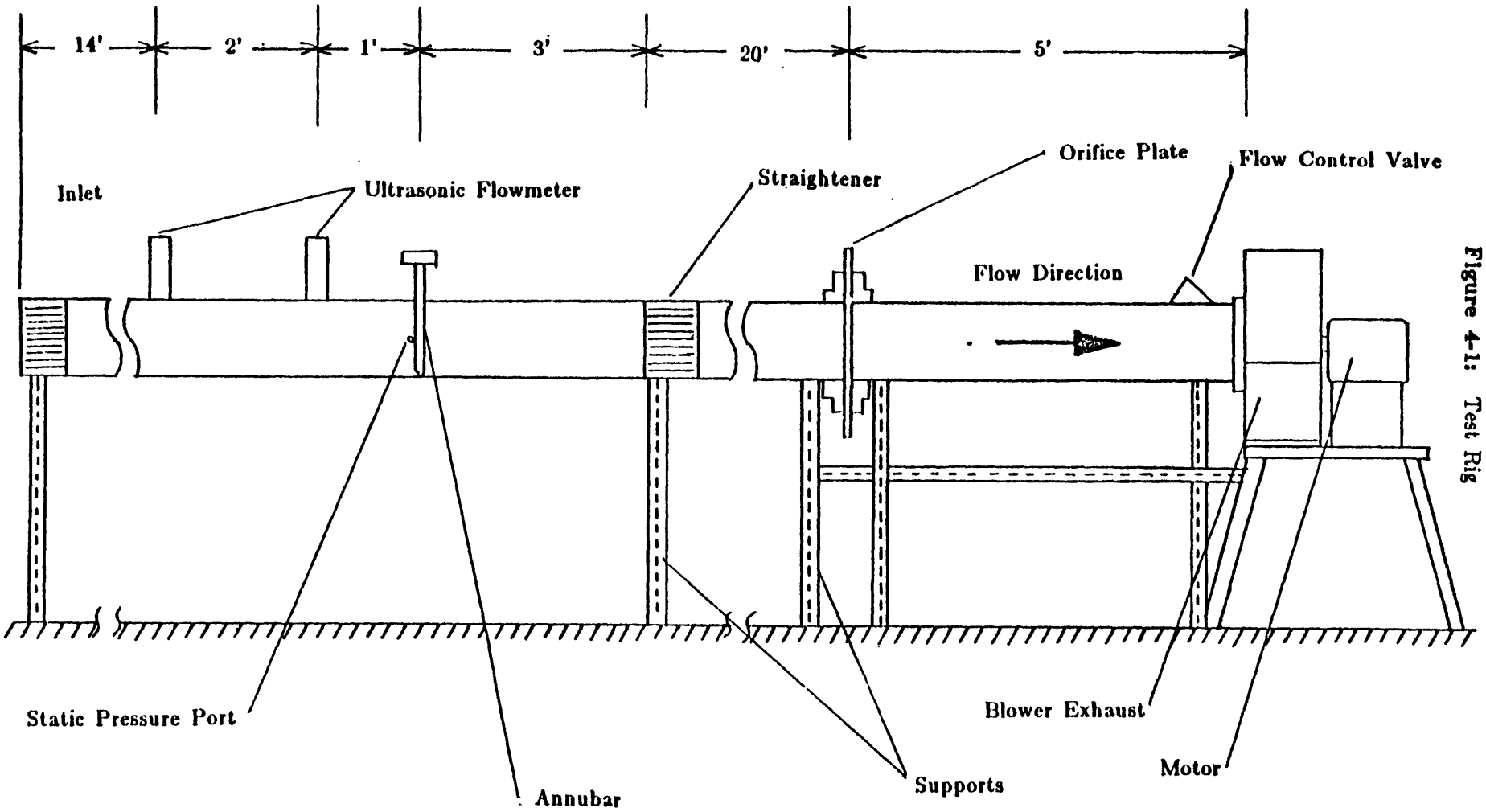

Figure 4-1: Test Rig

was used for the highest flow points. An inclined manometer with a range of 8 inches of water and a resolution of ±0.005 inches of water was used for low and medium flow points.

Thermometers with a resolution of ±0.25 degrees F were used for wet and dry bulb temperature measurements. Local barometric conditions were used as a basis for determining the static pressure and density of air.

The orifice flowmeter was installed in accordance with guidelines from ASME Report 6 on Fluid Flow Measurement. The expected accuracy of an installation of this nature is ±1.0 per cent [4].

4.4 Prototype Instrumentation

The acoustic pulses used to detect flowrate were observed using a Nicolet 206 digital oscilloscope. The oscilloscope is shown connected to the prototype in Figure 4-2. The Nicolet 206 has two input channels and stores information in digital form on floppy disks. Pulses were digitized and recorded at a rate of 1 MHz. The unit stored 4096 points per sweep, thus flight times up to 4.096×10^{-3} seconds were observed. The leading edges of the direct and reflected pulses had flight times less than 2.5×10^{-3} seconds. The remainder of the sweep captured the decay envelopes of the pulses.

As the acoustic pulse entered the pipe via one of the probes, it impinged on a piezoelectric crystal. The resulting electrical signal was sent to one channel of the oscilloscope. Signals on this channel were used to trigger the sweep. The other channel was used to record the pulse information received during the sweep by the other probe. The multiplexer permitted information from either the upstream or downstream probe to be observed on the recording channel. A delay on the order of 0.05×10^{-6} seconds occurs between the detection of the triggering signal and the start of a sweep. The magnitude of the delay is an unknown, constant quantity. The use of a single channel for recording both upstream and downstream pulses insured that the delay was constant for both directions.

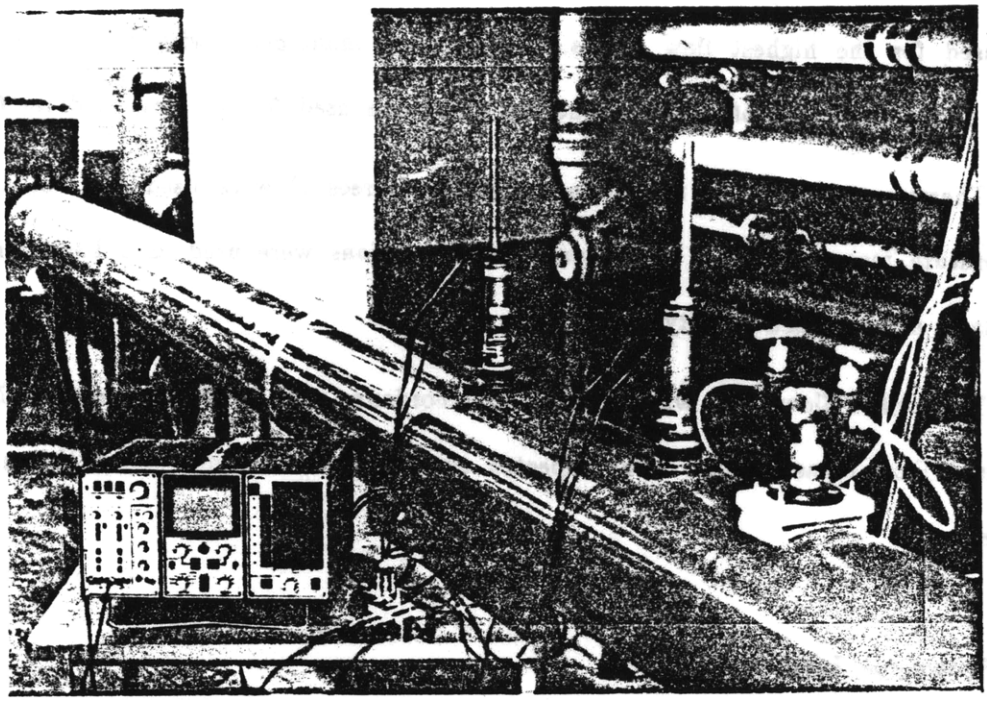

Figure 4-2: Prototype Installation

Shielded coaxial cable was used for all electrical connections to minimize the effects of noise on the signals.

4.5 Experimental Procedure

Hardware was tested in component form prior to assembly for installation in the test rig. Shock characteristics were determined. The device was assembled in a jig to test timing equipment. Finally, the prototype was installed in the rig for flow tests.

4.5.1 Component Testing

A probe was set up in a flat baffle so that the region immediately surrounding the probe tip was geometrically similar to the rig. Shock strength in the region of the probe tip was measured with a piezoelectric microphone. The information gathered was used to describe average shock strength and observe pulse consistancy.

Testing of the electronic components for short circuits, open circuits, effectiveness of the voltage clamp, etc. was performed at various stages of assembly using signal generators and analog oscilloscopes. Component and wiring problems were identified and rectified thus eliminating them as possible sources of error.

A number of support structures for the piezoelectric crystals were constructed and tested to determine the effects of mechanical vibrations. A compliant mount which effectively eliminated all mechanical noise above 15 kHz was used. Striking the assembly caused gross interference at low frequencies that could not be attenuated sufficiently by varying the mounting scheme. This effect was eliminated electronically through the use of the high pass filter.

4.5.2 Jig Testing

The probe pair was mounted in a jig for complete testing of the timing circuitry prior to flow testing. The jig held the probes in a configuration that was geometrically similar to their arrangement in the test rig. The probes were supported by stands at a height of one foot above the surface of a table. They were mounted perpendicular to the table and separated by a distance of two feet. The painted wood table top served as a reflective surface. No other acoustically reflective surfaces were in the vicinity of the jig.

Pulses were transmitted from one probe to the other. Transmission in both directions was performed. Direct and reflected components of the pulses were observed. The following adjustments were made to improve the performance of the unit. The electrical signals from the piezoelectric crystals was more than one order of magnitude stronger than expected. The gains of the preamplifiers were decreased to prevent saturation and improve frequency response. The position and orientation of the crystal were adjusted to improve clarity of the leading edges of the received signals.

Coarse, 09 mesh sandpaper was used as a rough reflective surface to examine possible

deterioration of the sharp leading edges. Shock strength was measured at the opening of the shock guide with a piezoelectric microphone. The sensitivity of this unit was -114 dB. Information was observed on a Tektronix storage oscilloscope.

4.5.3 Flow Measurement Testing

Probe mounting in the pipe was geometrically similar to the jig test configuration. Insertion depth was varied over a 0.25 inch range from a position where the center of the crystal coincided with the inside diameter of the pipe to a position where the the lowest point of the crystal was slightly outside this diameter. Best pulse behavior was obtained when the crystals were adjusted so their lowest points coincided with the pipe inside diameter.

Measurement of the flow involved examining 16 upstream signals and 16 downstream signals at each flowrate. Signal information was recorded on floppy disks for analysis later. All 32 signals were recorded over a 2 to 3 minute period. The following data acquisiton sequence helped verify constant flow over the interval during which measurements were taken.

1. Observe differential pressure across the orifice plate.
2. Fire and record 8 upstream pulses.
3. Fire and record 8 downstream pulses.
4. Repeat preceding steps.
5. Observe orifice plate differential pressure at end of sequence.

Flow was adjusted so that the points examined utilized the available range of the manometers.

Static pressure upstream of the orifice plate was determined by measuring the pressure difference between the upstream port and the local ambient pressure. This measurement was performed with the inclined manometer. Static pressure at the prototype location was

performed analogously using a dial manometer with a full scale differential presure range of 1 inch of water.

4.6 Data Analysis

The mass flow rates at the prototype location and the orifice meter were eqivalent. Flow measurements made with the two devices were compared in terms of the average velocity at the prototype location cross section. Data reduction for the devices are described.

4.6.1 Prototype Data Reduction

Received pulses stored on disks were individually examined to determine the arrival times of the direct and reflected components. Flight times were manually determined from observation of recorded signals. Occasional misfiring generated a number of clearly spurious signals which were rejected. Also, flight times greater than three standard deviations from the mean flight time were rejected. The discrimination between acceptable and unacceptable data conforms to the automated approach decribed in Section 3.3.

The sonic velocity was calculated using:

$$c = 49.02\sqrt{T} \tag{4.1}$$

where T is the temperature in degrees R and c is the sonic velocity in ft/sec [21].

Shock pressure rise at the opening of the shock guide was measured to be 2 psi, typically. This indicates a significant Mach effect. The average Mach factors for the L and S paths were calculated using Equation (3.13) and relevant geometric information. These factors were determined to be 1.0253 for the L path and 1.0192 for the S path.

Path lengths were calculated by taking the average of all flight times for all data points for the S and L paths respectively. Equations (3.4) and (3.5) were used and the respective Mach factors were applied to determine the path lengths.

A consistant difference between upstream and downstream flight times was observed during jig testing and under no flow conditions in the test rig. This difference was typically 25 microeconds for most test runs although one test run had a no flow transit time difference of about 10 microseconds. The flight times were on the order of 1680 microseconds for the L trajectory and 2380 microseconds for the S trajectory. Although the differences are small when compared to the flight times, they are significantly larger than the minimum resolveable time increment of 1 microsecond. The cause of this difference is believed to be mechanical in nature. Adjustments to the configuration of the probe tip affected the difference unpredictably. It should be noted that the acoustic pulses travel 0.32 inches in 25 microseconds. This dimension is on the order of the crystal size. Acoustic pulses impinged on the crystals at oblique angles. The leading edge of the pulse could interact with the crystal causing it to produce an electrical signal at some unpredictable time during the 25 microsecond interval. A flowmeter built for commercial service should have an electronic capability for adjusting and eliminating the no flow transit time difference. The difference could then be removed prior to installation.

The prototype did not have electronic difference cancelation capabilities. The no flow transit time difference was observed to be constant over each test run. The effect was eliminated from flow calculations by correcting the upstream and downstream flight times by an increment equal to half the measured transit time difference under no flow conditions.

The line averaged velocity, V, was calculated using Equation (3.2) and the S path flight times corrected for the no flow transit time difference. The profile correction factor, m, was calculated from Equation (3.3). The average velocity over the cross sectional area, V_{ave}, was calculated using:

$$V_{ave} = mV \tag{4.2}$$

4.6.2 Prototype Velocity Measurement Accuracy

Path length measurements were affected by a transit time offset between upstream and downstream pulses. Possible errors in average transit time measurement were considered to be as large as the no flow transit time difference. The average flight time for the L path was 1683 microseconds. The difference between upstream and downstream pulses at no flow was 25 microseconds, thus the possible error is 1.5 per cent. The average flight time for the S path was 2393 microseconds with a difference of 23 for a possible error of 1.0 per cent. These combine to produce a possible error of 3.5 per cent in the flow equation. Speed of sound error, calculated from the temperature resolution, is one order of magnitude smaller.

Minimum resolveable velocity is given by Equation (3.8). In some cases the transit time observed at one flowrate varied by as much as 8 microseconds. While this is extreme and many readings fell within 3 microsecond bands, it is conservative to use 8 microseconds as a minimum resolveable time increment. The minimum resolveable velocity is then 2.4 ft/sec.

4.6.3 Orifice Plate Data Reduction

Flow rates calculated with the orifice meter were calculated using:

$$Q = \{\pi d^2/4|\} \frac{C}{\sqrt{1-\beta^4}} \sqrt{2g_c h} \tag{4.3}$$

from References [4] and [22]. When expressed in terms of the average velocity at the prototype location, this equation becomes:

$$V_{ave} = 18.288 \frac{p_{so}}{p_{spro}} \beta^2 Y C \sqrt{\frac{h_w}{\rho\{1-\beta^4\}}} \tag{4.4}$$

where:

- $g_c = 32.174 \frac{\text{ft-lbm}}{\text{lbf-sec}^2}$ (Conversion Constant).
- β = Ratio of orifice diameter to pipe diameter (dimensionless).
- C = Coefficient of discharge (dimensionless).

- h = Effective differential pressure (ft of working fluid).
- h_w = Pressure differential (inches water).
- ρ = Air density (lbm/ft^3).
- Y = Expansion factor (dimensionless).
- Q = Volume flow through orifice (ft^3/sec).
- d = Orifice diameter (inches).
- p_{so} = Static pressure at orifice plate (in Hg).
- p_{spro} = Static pressure at prototype location (in Hg).

The density of air, ρ, was calculated using [3]:

$$p_e = 0.000296T_w^2 - 0.0159T_w + 0.41 \tag{4.5}$$

$$p_p = p_e - p_b\{T_d - T_w\}/2700 \tag{4.6}$$

and

$$\rho = \frac{70.73(p_b - 0.378p_p)}{R(T_d + 495.70)} \tag{4.7}$$

where:

- $R = 53.35 \frac{\text{ft-lbf}}{\text{lbm-degree R}}$ (gas constant).
- T_d = Dry bulb temperature (degrees F).
- T_w = Wet bulb temperature (degrees F).
- p_e = Saturation vapor pressure (in Hg).
- p_p = Partial pressure (in Hg).
- p_b = Barometric pressure (in Hg).

The barometric pressure used in these equatons was found by subtracting the measured pressure difference between ambient and static pressure upstream of the orifice plate from the local barometric pressure. The values of C and Y were obtained graphically from the references.

4.6.4 Orifice Plate Velocity Measurement Accuracy

The overall accuracy of the orifice flow measurements is given by the equation for combining tolerances [6]:

$$X = \pm\sqrt{(n_1X_1)^2+(n_2X_2)^2+...+(n_kX_k)^2} \tag{4.8}$$

where:

- X = Overall tolerance.
- X_k = Tolerance of individual factor.
- n_k = Exponent of the factor.

The tolerance of β is limited by the precision of the pipe inside diameter. The 11.84375 inch average I.D. was found to be consistant to within $\pm 1/32$ inches or ± 0.26 per cent. Combining this with a ± 0.001 inch tolerance of the orifice diameter gives a tolerance for β of ± 0.27 per cent. Evaluating over the possible range of β gives a tolerance of ± 0.05 per cent for the $(1-\beta^4)$ term. Combining a resolution of $\pm$ 0.005 inches of water and uncertainty of water density of 0.1 per cent gives a tolerance for h_w of ± 0.6 per cent. The ASHRAE tables indicate that the accuracy of ρ is ± 0.5 per cent. The tabular information for C is accurate to ± 1.0 per cent [4]. The graphical information for Y is accurate to ± 0.05 per cent.

Applying Equation (4.8) to the above mentioned tolerances suggests an overall accuracy of orifice flow measurement of ± 1.2 per cent. The differential pressure showed oscillations on the order of the resolution of the inclined manometer (± 0.005 inches water). The middle value of the oscillations was used.

It should be noted that questions about the accuracy of orifice plates in general have been raised. It has been suggested that systemic errors on the order of 2 per cent exist for large volume gas flow measurements. These errors are expected to occur in particular where extrapolated values of the discharge coefficient are used [10]. The orifice meter was used as a reference in this work because it is widely accepted as a standard in the natural gas industry.

Chapter 5

Results

A comparison between flow measurements made with the ultrasonic flowmeter and the orifice meter is shown in Figure 5-1. The agreement of the results falls within the uncertainty of a minimum resolveable velocity of 2.4 feet per second predicted in Chapter 4. Data from which the points were determined are listed in Appendix C. The goal of an accuracy of ±0.5 per cent for a commercial flowmeter could not be met with the timing equipment employed for prototype testing.

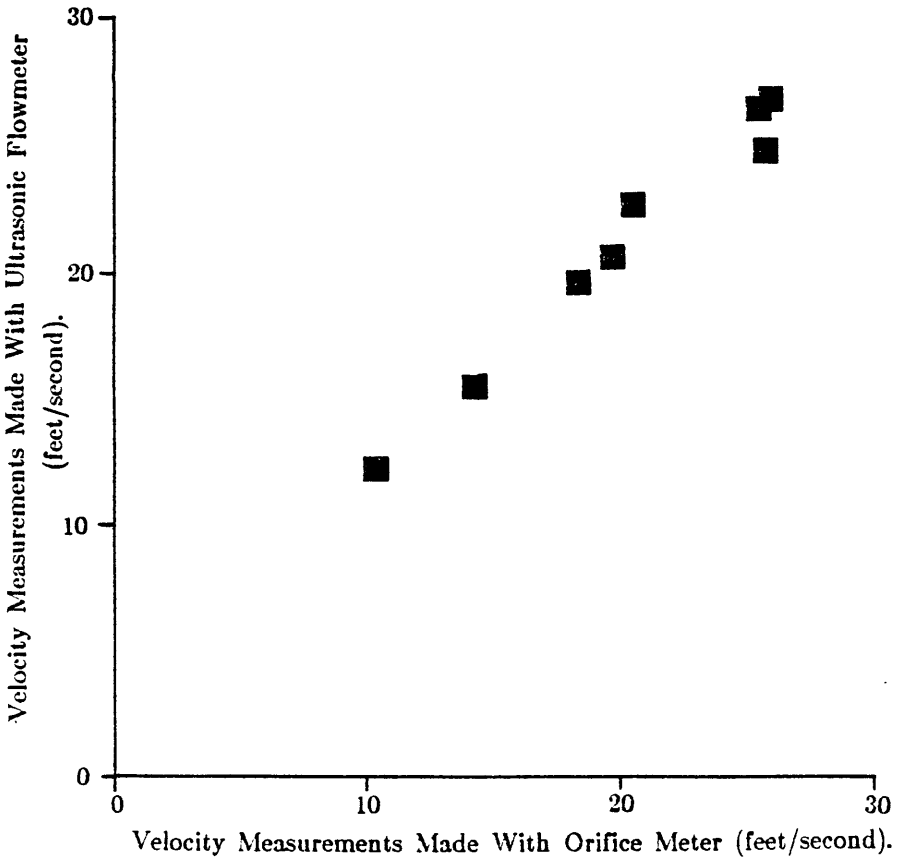

Figure 5-1: Ultrasonic Flowmeter v.s. Orifice Meter

The following characteristics were observed during jig and test rig experiments:

1. The pipe diameter calculated from ultrasonic time of flight measurements was 11.73 inches. The diameter at the prototype location was measured with calipers to be 11.81 inches. This discrepancy falls well within allowable limits of experimental accuracy.

2. Orientation of the crystal affects the clarity of the leading edges. Best pulse behavior was defined as a sharp leading edge on the S path pulse component. This was obtained when the crystal was mounted normal to the flight direction of the S pulses. This orientation of the crystal degrades the character of the L pulse leading edge because the L pulse strikes the crystal at an oblique angle. This trade off was found to be acceptable because the L path information is used only for calibration while the S path information is used for calibration and flow measurement and is, therefore, more critical.

3. In jig testing, the quality of the reflective surface had no noticeable effect on the behavior of the pulses. A wood table top and 09 mesh sandpaper were used as reflective surfaces. This supports the hypothesis that a leading edge blurred by reflection off of an irregular surface becomes sharp again as a consequence of the steepening phenomena associated with shock waves.

4. A large S strength to L strength ratio was obtained by retracting the crystals into the probe tip. The cause of this phenomena is believed to be refractive losses in the L pulse.

5. A substantial difference in transit times between pulses fired in opposite directions under no flow conditions was observed in jig tests and in the flow test rig. The difference was repeatable and consistant over each test run and reversed sign when the upstream and downstream probes were switched. The offset was associated with pulse direction with respect to the probes regardless of probe orientation. The magnitude of this difference was typically on the order of 25 microseconds. The source of this phenomena is believed to be mechanical in nature in that adjustment to the probe tip configuration affected the transit time difference. The angle at which the leading edge of an acoustic pulse impinges on the crystal is also believed to affect this difference.

The behavior of the pulses is illustrated in Figure 5-2. The direct and reflected components are easily identified. The initial transient is the L pulse leading edge, the second transient is the S pulse leading edge, and the expanding envelope after the S pulse is caused by spurious reflections. The same pulse is shown in its entirity and expanded at the L component and S component arrival times.

Figure 5-2: Pulse Characteristics

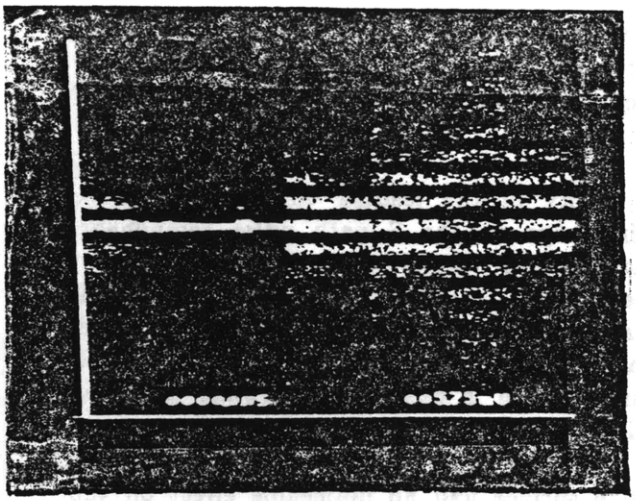

Typical Trace
Sweep duration: 4096 μsec.; Vertical range: ± 100mV.
Note sharp leading edges of L pulse (first transient)
and S pulse (second transient).

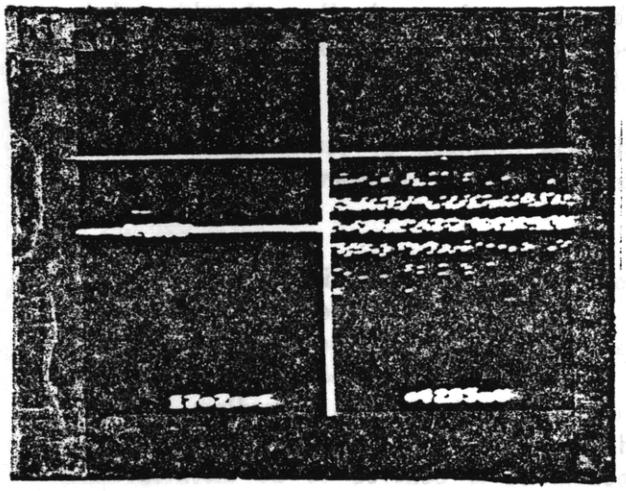

Above trace expanded at L pulse time of arrival.
Cursors indicate time (1707 μsec) and strength (42.85 mV)
of L pulse leading edge. Scale: 1024 μsec of sweep shown.

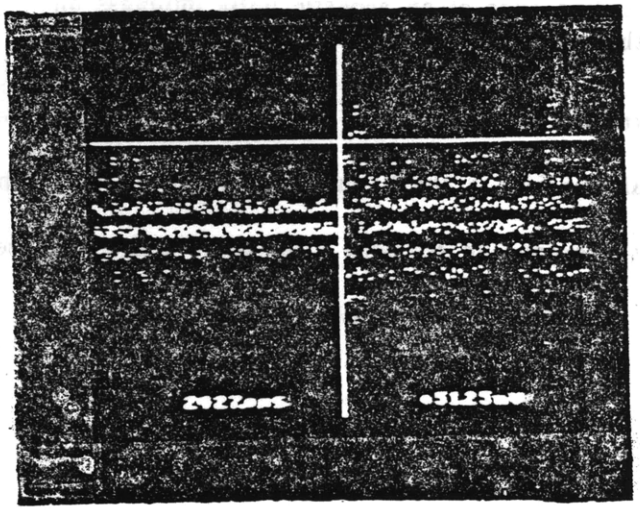

Above trace expanded at S pulse time of arrival.
Cursors indicate time (2427 μsec) and strength (51.25 mV)
of S pulse leading edge. Scale: 1024 μsec of sweep shown.

Chapter 6

Conclusions and Recommendations

The feasibility of using direct and reflected acoustic pulses to determine calibration dimensions and perform flow measurements was demonstrated. Several significant areas that must be addressed in the continuation of this program were identified. They include:

1. Development of a suitable pulse generator.
2. Implementation of a dedicated data acquisition and control system.
3. Isolation and quantification of the geometric factors affecting flow measurement. The region in the vicinity of the transducers is particularly critical.
4. Development or selection of optimal transducers.
5. Experimental examination of the effects of distorted flow profiles on the performance of the flowmeter.
6. Effects of a high pressure natural gas environment on the life and performance of the flowmeter.
7. Identification and elimination of the source and effects of the transit time difference observed under no flow conditions.

References

[1] Alles, David.
Design and Development of a Fast Acting Valve for Plasma Research.
Master's thesis, MIT, 1963.

[2] *Annubar Flow Measurement - Industrial Line*
Dietrich Standard Corporation, Boulder, Colorado 80301, 1978.

[3] ASHRAE Std 51-75.
Laboratory Methods of Testing Fans for Rating Purposes.
Technical Report, American Society of Heating, Refrigerating, and Air Conditioning Engineers, 1972.

[4] Bean, Howard S.
Fluid Meters, Their Theory and Application.
Technical Report 6, American Society of Mechanical Engineers, 1971.

[5] Bruner, Robert S.
Theoretical and Experimental Assesment of Uncertainties in Non-intrusive, Ultrasonic Flow Measurement.
In *Proceedings of the Symposium on Flow Measurement in Open Channels and Closed Conduits.* NBS, 1977.

[6] Clark, W.
Flow Measurement by Square Edged Orifice Plates Using Corner Taps.
Pergamon Press, 1965.

[7] Continos, Costas.
Information on large volume flow measurement presented at review meeting.
Jan, 1982.

[8] Continos, Costas.
Letters to D. Bender; Dec 10, 1981 and Jan 7, 1982.
Contains description of application and program objectives.

[9] Cook, F. Bert and Moffatt, E..
Flow Meter for High Pressure Gas Using Sonic Pulses.
In *Advances in Instrumentation.* ISA International Instrumentation and Automation Conference, Oct, 1974.

[10] Day, Raymond.
Conversations with author re: Gas Research Institute studies.
1982.

[11] Gooberman, G. L.
Ultrasonics Theory and Application.
Hart Publishing Co., New York, 1968.

[12] Hastings, C. R.
The Leading Edge Acoustic Flowmeter - An Application to Discharge Measurement.
Journal of the New England Water Works Association , 1970.

[13] Hickman, William.
Annubar Properties Investigation.
In *Advances in Instrumentation.* ISA Industry Oriented Conference and Exhibit, October, 1975.

[14] Mason and Thurston (editor).
Ultrasonic Flowmeters.
Academic Press, 1979.

[15] McMorris, John A.
Design of an Underwater Explosion Simulator.
Master's thesis, MIT, 1963.

[16] McShane, J.L.
Ultrasonic Flowmeters.
In *Advances in Instrumentaion.* ISA International Instrumentation and Automation Conference, Oct, 1974.

[17] Moffatt, E. and Fetterhoff, K.
Large Volume Flow Measurement By Sonic Techniques.
In R.E. Wendt Jr. (editor), *Flow - Its Measurement and Control in Science and Industry,* . ISA, 1974.

[18] Ogata, Katsuhiko.
Modern Control Engineering.
Prentice - Hall, Inc., New Jersey, 1970.

[19] Pederson, Bradshaw, Lynnworth, and Morel.
New Ultrasonic Flowmeter for the Natural Gas Industry.
In *Proceedings of the Symposium on Flow Measurement in Open Channels and Closed Conduits.* NBS, 1977.

[20] Selby, Samuel.
CRC Standard Mathematical Tables.
Chemical Rubber Co., 1973.

[21] Shapiro, Ascher H.
The Dynamics and Thermodynamics of Compressible Fluid Flow.
John Wiley and Sons, New York, 1953.

[22] Stearns, Reid F.
Flow Measurement with Orifice Meters.
Van Nostrand, 1962.

[23] Williams, Albert and Tochko, John.
An Acoustic Sensor of Velocity for Benthic Boundary Layer Studies.
Technical Report 3843, Woods Hole Oceanographic Institute, 1981.

[24] Zel'dovich, Ya. B. and Raizer Yu. P.
Physics of Shock Waves and High Temperature Hydrodynamic Phenomena.
Academy of Sciences, Moscow, 1967.

Appendix A
The Annubar Flow Sensor

The Annubar (tm) is a dynamic head device made by Dietrich Standard. This unit is presently employed by Consolidated Edison for measurement of interdistrict gas flow. The design and operation of this unit were studied. Flow tests were performed.

A.1 Background

The design of the Annubar, shown in Figure A-1, is based on the combined reversed Pitot tube concept described in ASME Report 6 [3]. The device has four upstream ports which sense the impact pressure and one downstream port that senses a suction pressure. The upstream ports open into a common cavity. Fluid velocity is infered from the difference between pressure measured at the midpoint of the impact pressure cavity and the rear facing suction port [2].

Port spacing was arranged so that each port samples points representing equal annular areas. Since the impact pressures vary between ports, there is flow into and out of the impact pressure cavity. Research on the effect of this non-zero internal flow condition on the relationship between the measured pressure difference and actual flowrate has shown that the Annubar output can only be predicted for the case of fully developed, axi-symetric turbulent flow without swirl in a smooth pipe [7]. Calculation of the behavior of the impact pressure sensing method under non-ideal conditions is much more difficult and depends greatly on the exact nature of the flow conditions.

The suction port of the Annubar is located at the midpoint of the trailing edge. The cross section at this point is a sharp edged diamond shape. Analysis of differential pressure

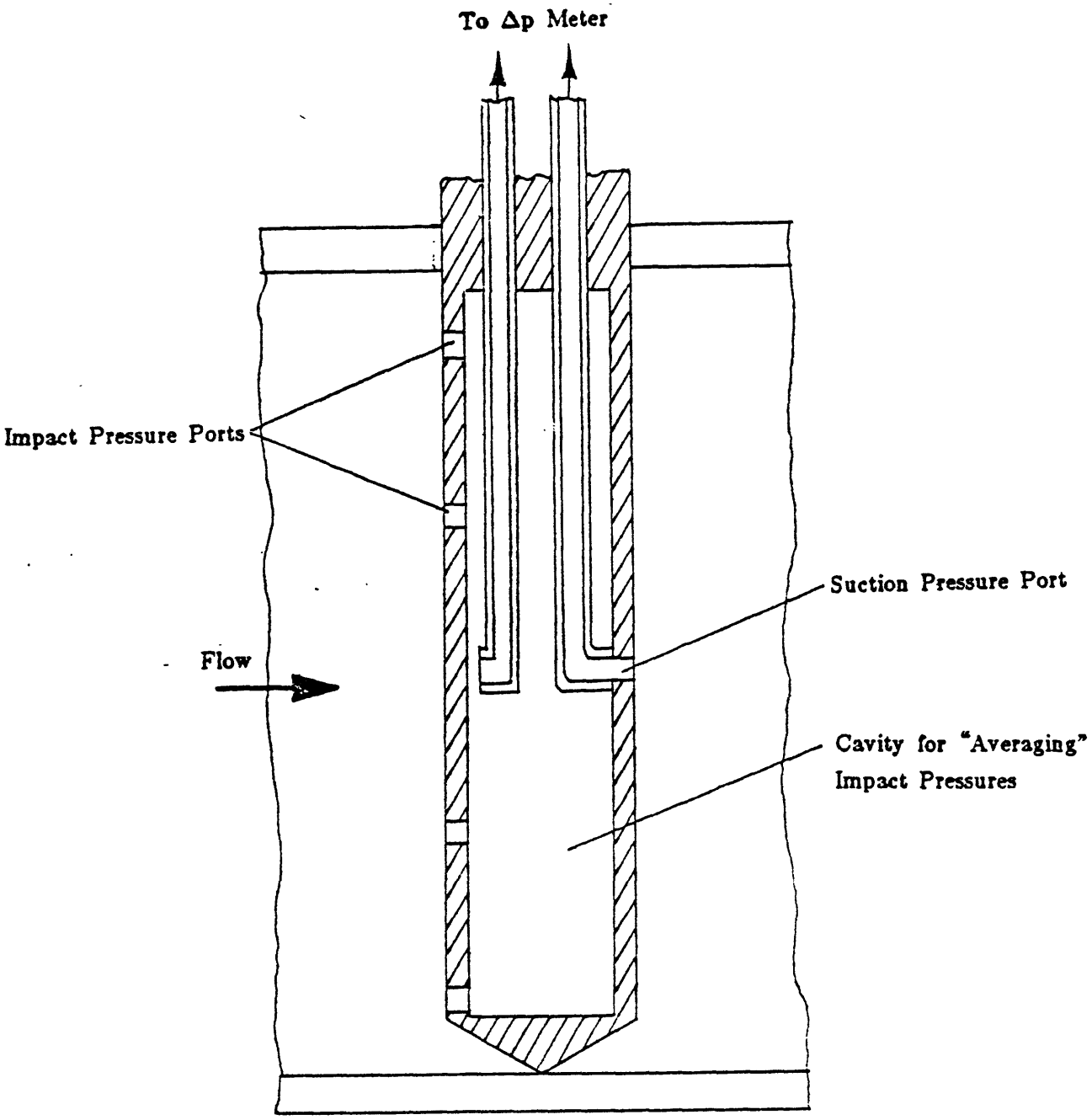

Figure A-1: Annubar Flow Sensor

measurements are derived using the base pressure coefficient at this point. It should be noted that the suction port is located in a region where vortex shedding causes appreciable variation in the local suction pressure [5].

A.2 Application Information

The Annubar is used in conjunction with Bristol Instruments differential pressure transducers. The range of the differential pressures measured is 0 to 5 inches of water. The manufacturer claims an accuracy of ±0.2 per cent of full scale. The Annubar units are typically installed with 7 diameters of straight upstream pipe and three diameters of straight downstream pipe. Two units are used at each metering point to cover bidirectional flow. One unit is installed in series with an orifice metering station. The unit at this location tracks the orifice plate measurements within specified accuracy levels. One Annubar is installed within 2 diameters of an elbow [4].

In one case, it was reported that an Annubar removed from service for routine inspection was found to have all impact ports clogged. The flow measurements made with this unit over the period following its most recent previous inspection failed to indicated any anomaly [4].

A.3 Flow Measurement Testing

An Annubar, provided by Charles Britton of Dietrich Standard was installed at the location of the ultrasonic flowmeter prototype for testing. Two dial manometers were used for differential pressure measurements. The ranges of these gages were 0 to 1.0 and 0 to 0.5 inches of water with resolutions of ±0.01 and ±0.005 inches of water respectively. A port at the Annubar location, indicated in Figure 4-1, was used to sense the static pressure. Three differential pressures were observed directly:

- $\Delta p_{i,sc}$ = Pressure difference between impact and suction ports.
- $\Delta p_{i,st}$ = Pressure difference between impact and static ports.
- $\Delta p_{st,sc}$ = Pressure difference between static and suction ports.

Flow was calculated using equations in the Annubar handbook [1]:

$$Q_A = C'\sqrt{h_w} \tag{A.1}$$

which, expressed in terms of average velocity at the Annubar location, becomes:

$$V_{A,ave} = \{\pi C'/4D^2\}\sqrt{h_w} \tag{A.2}$$

where:

$$C' = F_{NA}KD^2F_{RA}Y_AF_MF_{AA}F_1\sqrt{1/\rho_f} \tag{A.3}$$

The constants in Equation (A.3) are defined and specified in Reference [1]. Note that the D^2 term cancels out of Equation (A.2). A conversion factor of $144 in^2/ft^2$ must be included. The values of these constants are:

- F_{NA} = 5.9823 (Units conversion)
- ρ = Air density, lbm/ft^3 (From Equation (4.7))
- K = 0.7039, dimensionless (Flow coefficient)
- F_1 = 1.0, dimensionless (Altitude correction factor)
- F_{AA} = 1, dimensionless (Thermal expansion factor)
- F_M = 1, dimensionless (Manometer factor)
- Y_A = 0.998, dimensionless (Blockage ratio factor)
- F_{RA} = from .960 to .983, dimensionless (Reynolds number factor)

Thus Equation (A.2) is reduced to:

$$V = 12.842F_{RA}\sqrt{\Delta p_{i,sc}/\rho} \tag{A.4}$$

where $\Delta p_{i,sc}$ is the differential pressure in inches of water.

A.4 Results and Observations

Flow measurements made with the Annubar are compared to the orifice meter results in Figure A-2. Oscillations of $\Delta p_{i,sc}$ had a magnitude of 4 to 6 per cent of the measured value. Oscillations of $\Delta p_{st,sc}$ were of a comparable magnitude. The $\Delta p_{i,st}$ measurements showed no oscillatory behavior. This indicates significant pressure fluctuation at the suction port.

Under normal conditions this phenomena made accurate differential pressure measurements impossible. The suction pressure line was throttled to dampen the oscillations. The value of the differential pressure observed with the throttled suction pressure line was used in the flow calculations.

The accuracy of the flow measurements made with the Annubar is determined by applying Equation (4.8) to the tolerances for $\Delta p_{i,sc}$ given above and ρ given in Chapter 4. The level of accuracy obtained thusly is ± 2.1 per cent at a velocity of 25 feet per second and $\pm$ 3 per cent at 15 feet per second. Combining these tolerances with the tolerance of ± 1.2 per cent obtained for the orifice meter in Chapter 4 gives an uncertainty of the relationship between orifice plate and Annubar measurements of ± 3.3 and ± 4.2 per cent at flow rates of 25 and 15 feet per second respectively.

Most measurements made with the Annubar agreed with those of the orifice meter within the prescribed tolerance. The failure of some points to fall within the specified uncertainty is believed to arise from effects of the vortex oscillations.

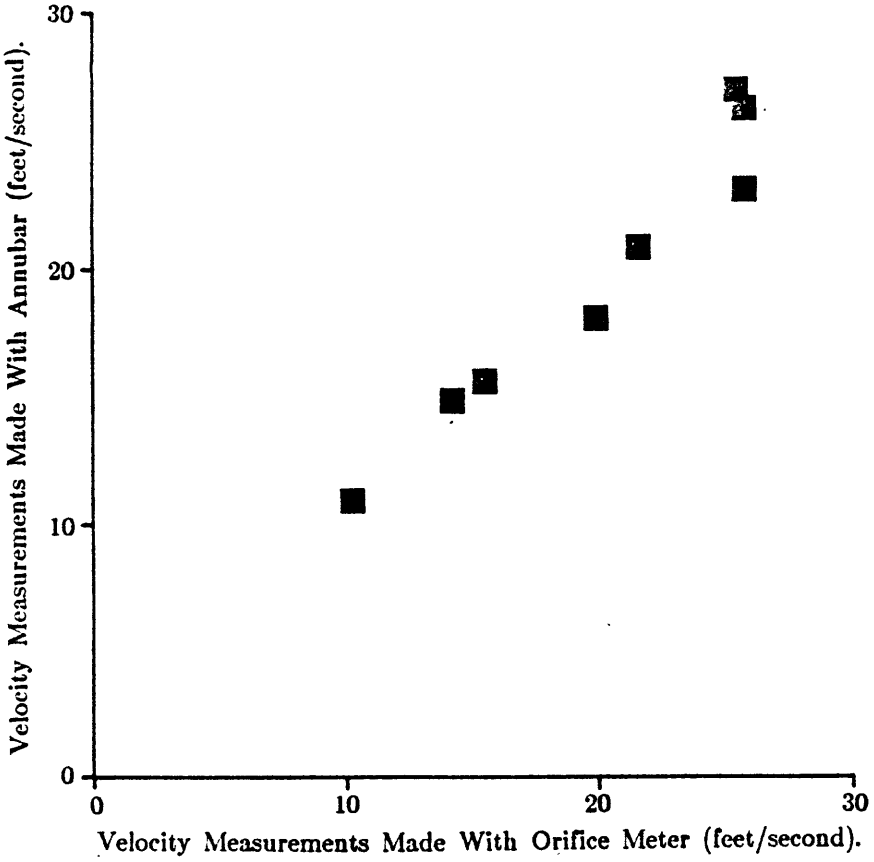

Figure A-2: Annubar v.s. Orifice Plate Flow Measurement

Appendix B
Alternative Flowmeters

Various flowmetering techniques were considered prior to the selection of an ultrasonic method for further study. The most viable candidates included turbine meters and other ultrasonic devices.

B.1 Internally Assembled Turbine Meter

A possible, almost totally mechanical, option was the design of a turbine meter that could be installed through small openings in the line. The concept is illustrated in Figure B-1.

The centerbody of the device would be inserted individually through a conventional flange tap and supported externally. It would be possible to support the centerbody at several points through the use of multiple openings. The centerbody would have two spindles capable of rotating freely with respect to one another. Blades would be inserted through openings adjacent to the support and attatched sequentially to the spindles.

Two sets of blades would be used eliminating the need for flow straighteners. The blade sets would rotate in opposite directions. The blades would be designed with symetric airfoil shapes and be twisted to provide uniform angles of attack with respect to the flow direction. The use of symetric airfoil; cross-sections permits operation in bidirectional flow. The blades would be twisted in opposite directions so that they would be counter rotating. This arrangement offsets the effects of swirl. The presence of swirl would affect the rotational speed of both blade sets equally. Flow rate would be proportional to the difference of rotational speeds of the two blade sets.

The dual blade set concept has been implemented successfully in high accuracy

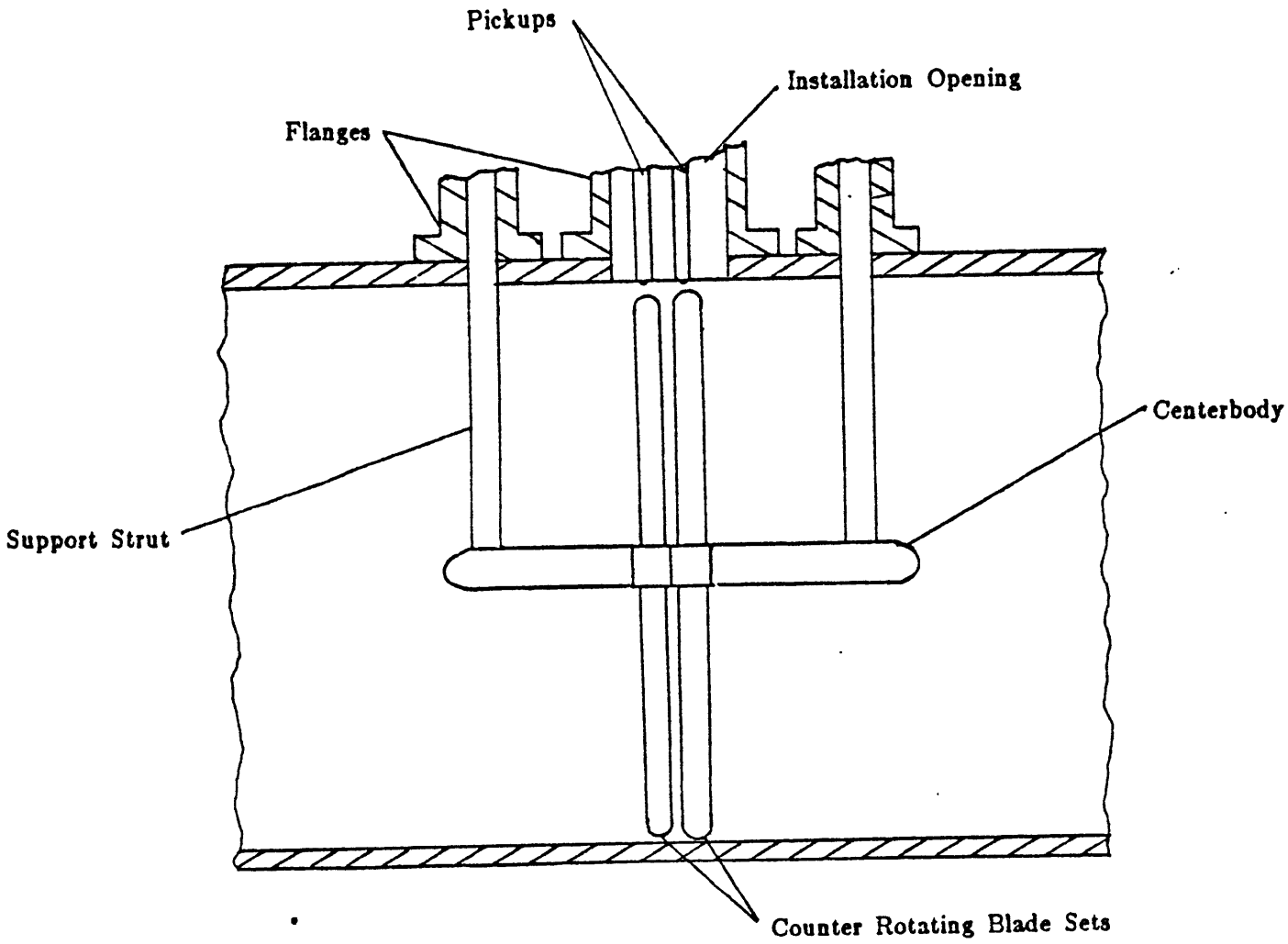

Figure B-1: Internally Assembled Turbine Flowmeter

commercial applications for fully enclosed turbine meters. However, internal assembly poses some special problems. For instance, in a fully enclosed turbine meter the clearance between the rotors and the shroud is precisely determined. The internally assembled turbine meter uses the pipe wall as a shroud. Since it is desireable to minimize the blade to shroud clearance to eliminate tip effects and interogate the entire cross-section of the flow area, the centerline must be located accurately. Moving parts could be fouled by particles entrained in the gas stream. Also, scale accumulations could affect tip clearance in an unpredictable

manner. In light of the difficulties of implementing this concept, it was decided to pursue an approach relying less heavily on critical moving parts.

B.2 Alternative Ultrasonic Devices

Significant research on the measurement of fluid flows with sonic methods has been performed for some twenty years [8], [9]. Unfortunately, most of this work has dealt with liquid flows. It is easier to generate high frequency tonebursts which persist for great distances with low powered sonar type transducers in liquids. This is much more difficult for gases as a consequence of the generally poor acoustic coupling between solid and gas [6]. Thus much liquid flowmeasuring technology is inapplicable to the problem at hand. In particular, devices employing externally mounted transducers and transmission paths through pipe walls are well developed for liquids but totally unsuitable for gases.

A number of devices employing acoustic techniques have been developed for gas flows. The existing approaches which are suitable for large volume gas flow measurement may be categorized on the basis of configuration and technique as follows:

1. Techniques:

    a. Phase shift measurement with a reference: The phase angles of single or counterpropagating waves of constant frequency change with velocity and are measured with respect to an internal reference.

    b. Phase shift without reference: The changes in phase angle of counterpropagating waves are measured with respect to each other.

    c. Time of flight: Velocity is determined by measuring flow induced changes in transit time of pulses. Typically, only counterpropagating signals are used.

2. Configuration:

    a. Dual Trajectory: Two or more signal paths are used. Pulses travel along individual paths in one direction only. The paths may be oriented for either upstream or downstream propagation.

b. Common trajectory: Both upstream and downstream flight directions are used for each signal path.

c. Multiple path: A combination of dual or common trajectories is used to interogate flow at several places in the cross section.

d. Single path: The cross section is interogated along one path. This is only possible for common trajectories.

The simultaneous use of a reflecting and direct components of an acoustic pulse has not been previously examined.

The requirements of the application discussed in Chapter 2 preclude the use of many previously developed methods. First, the limitation of access to a small section of the circumference of the line prohibits the use of diametrically opposed transducers. A reflected trajectory is called for. In order for a reflected signal to preserve its frequency information, the the wavelengths of concern must be significantly larger than purturbations on the reflecting surface. For example, the most nearly commercially viable approach to date is found in an opposed transducer configuration device using phase shift measurement [10], [11]. This device has achieved high accuracy in field tests using a 100kHz signal as a carrier for phase information. The successful reflection of this signal would require surface disturbances to be several times smaller than the wavelength of 0.13 inches. Since surface roughness of this order is inevitible it would be difficult to implement a device of this type here. Second, intrinsic calibration of the device is necessary as a consequence of the lack of a priori flow information. This requires that the actual path lengths be determined after installation. This information is difficult to extract from simple phase measurements. No technique for obtaining the path length information from phase shift measurements has been published to date.

B.3 Other Alternatives

Many other methods of flow measurement were considered. These are listed in table B-I along with their operating principles, advantages, and disadvantages.

Table B-I: Alternate Methods of Flow Measurement

Pitot Tube Array

Principle:	Measuring the total pressure at many points would give an accurate average velocity. Measurement points must be properly distributed. An integrating manometer could average the pressures.
Advantages:	Off shelf components.
	Low power consumption.
	No pipe length.
Disadvantages:	Difficulty of mechanizing an adequate manometer.
	Looses accuracy at low flow.
	Sensitive to fouling.

Insertion Turbine Meter

Principle:	A conventional flowmeter with proven accuracy would be used. The unit would be inserted through a relatively large opening in the line and be anchored by an inflated or internally assembled collar.
Advantages:	Turbine flowmeters have acceptable accuracy.
	Short pipe length.
	Flow would be accelerated by the reduction in area due to the collar. Low flow sensitivity is increased, sensitivity to skewed profiles is decreased.
Disadvantages:	Supports could cause high head losses.
	Mechanization of the support would may complicate installation.

Insertion Flow Straighteners

Principle:	A fix for the present system. Straighteners could be deployed inside the pipe in an umbrella-like fashon.
Advantages:	Uses existing measurement device.
	Siplicity.
Disadvantages:	Difficult to install.
	Generates head loss.
	Does not improve accuracy at low flowrates.
	Removes swirl but does not provide a uniform or axisymetric flow profile.

Collapsible Laminar Flow Element

Principle:	A conventional laminar flow element arrangement would be deployed and anchored in the line. Flow would be ducted through many parallel tubes so that the flow regime would be laminar and predicted accurately according to well established laws.
Advantages:	Simple principle.
	Can be made accurate at low flow rates.
Disadvantages:	Head loss makes good anchoring nessecary.
	Head loss may be unacceptably high.
	Irregular flow profile could degrade accuracy.

Doppler Effect

Principle:	A Doppler shift could be generated between a fixed receiver and particles entrained in the stream.
Advantages:	High accuracy is possible.
	Off shelf components could be used.
Disadvantages:	A significant quantity of particles must be suspended in the stream at all times.

Temperature Effect

Principle: Temperature rise across a flow restriction would be measured.

Advantages: Simple principle.

Disadvantages: Temperature difference would be extremely small and difficult to measure accurately.

Variable Orifice

Principle: The area of an internally mounted orifice is varied to maintain a constant pressure drop. Flow would be a function of orifice size. Force to drive the expansion and contraction of the orifice would be derived from the pressure drop.

Advantages: Sensitivity increases at low flow.

Disadvantages: Complicated mechanization and installation.

Hot Wire Anemometer Array

Principle: Velocity would be measured at many points with good accuracy. An accurate average velocity at the cross section could be determined.

Advantages: Off shelf components.

Ease of installation.

No pipe length.

No danger of combustion in a pure methane environment.

Velocity is measured directly.

Disadvantages: Consumes more power than alternatives.

Even though there is no danger of combustion, the idea would probably seem too radical to the gas industry.

Pressure Drop Over Known Length

Principle: A long tube is inserted into a straight section of the main. Flow is determined by measuring the pressure drop. Pressure drop would be measured by connecting both endes of the tube to a manometer.

Advantages: Simple.

Easy to install.

Pressure drop is readily measured.

Disadvantages: The pipe diameter and surface condition must be known accurately.

Sufficient lengths of straight, uniform, and uninterupted pipe must be available.

Appendix C
Data

Data gathered from the flow tests of the ultrasonic prototype are listed below. Each measurement point includes all orifice plate information and a list of observed flight times.

- T_D = Dry bulb temperature (degrees F).
- T_W = Wet bulb temperature (degrees F).
- P_B = Barometric pressure (inches Hg).
- Δp_o = Orifice plate differential pressure (inches water).
- δp_o = Static pressure depression at orifice (inches water).
- δp_p = Static pressure depression at prototype (inches water).
- t_{ul} = L path upstream flight time (10^{-6} seconds).
- t_{us} = S path upstream flight time (10^{-6} seconds).
- t_{dl} = L path downstream flight time (10^{-6} seconds).
- t_{ds} = S path downstream flight time (10^{-6} seconds).

Point A

$T_D = 78$ $T_W = 65$ $P_B = 30.51$ $\Delta p_o = 7.50$
$\delta p_o = 1.4$ $\delta p_p = .80$

t_{ul}	t_{us}	t_{dl}	t_{ds}
1695	2419	1670	2371
1695	2421	1673	2371
1694	2418	1669	2368
1695	2420	1669	2368
1696	2420	1669	2367
1695	2417	1669	2371
1695	2419	1669	2370
1695	2419	1670	2369

Point B

$T_D = 78$ $T_W = 65$ $P_B = 30.51$ $\Delta p_o = 4.75$
$\delta p_o = .93$ $\delta p_p = .42$

t_{ul}	t_{us}	t_{dl}	t_{ds}
1688	2408	1677	2377
1691	2413	1677	2377
1690	2409	1677	2377
1691	2414	1673	2369
1687	2410	1678	2376
1691	2412	1675	2374
1691	2412	1672	2371

Point C

$T_D = 78$ $T_W = 65$ $P_B = 30.51$ $\Delta p_o = 4.45$
$\delta p_o = .91$ $\delta p_p = .40$

t_{ul}	t_{us}	t_{dl}	t_{ds}
1693	2413	1677	2380
1690	2410	1677	2377
1687	2409	1679	2377
1690	2414	1676	2377
1689	2409	1674	2377
1691	2414	1674	2377
1689	2411	1677	2380

Point D

$T_D = 78$ $T_W = 65$ $P_B = 30.51$ $\Delta p_o = 2.34$
$\delta p_o = .6$ $\delta p_p = .25$

t_{ul}	t_{us}	t_{dl}	t_{ds}
1685	2405	1682	2387
1687	2406	1683	2387
1687	2405	1683	2387
1687	2406	1682	2386
1685	2405	1680	2385
1687	2406	1682	2386
1687	2406	1680	2384

Point E

$T_D = 78$ $T_W = 65$ $P_B = 30.51$ $\Delta p_o = 1.23$
$\delta p_o = .36$ $\delta p_p = .20$

t_{ul}	t_{us}	t_{dl}	t_{ds}
1684	2401	1688	2395
1684	2400	1686	2393
1685	2404	1688	2394
1685	2404	1689	2394
1687	2409	1689	2392
1690	2409	1688	2392
1686	2405	1688	2394

Point F

$T_D = 78$ $T_W = 65$ $P_B = 30.51$ $\Delta p_o = 0$
$\delta p_o = 0$ $\delta p_p = 0$

t_{ul}	t_{us}	t_{dl}	t_{ds}
1669	2375	1694	2399
1669	2375	1694	2402
1671	2375	1694	2400
1669	2375	1692	2394
1667	2375	1694	2397
1667	2373	1691	2394

Point G

$T_D = 77$ $T_W = 62$ $P_B = 30.42$ $\Delta p_o = 7.62$

$\delta p_o = 1.4$ $\delta p_p = .81$

t_{ul}	t_{us}	t_{dl}	t_{ds}
1687	2419	1644	2357
1687	2417	1637	2351
1688	2412	1646	2358
1689	2417	1658	2356
1689	2415	1656	2355
1689	2416	1656	2356
1687	2416	1654	2360

Point H

$T_D = 77$ $T_W = 62$ $P_B = 30.42$ $\Delta p_o = 4.86$

$\delta p_o = .96$ $\delta p_p = .40$

t_{ul}	t_{us}	t_{dl}	t_{ds}
1689	2411	1639	2361
1690	2412	1639	2361
1690	2411	1639	2361
1686	2411	1639	2361
1686	2410	1639	2359
1683	2411	1639	2362

Point I

$T_D = 77$ $T_W = 62$ $P_B = 30.42$ $\Delta p_o = 0$
$\delta p_o = 0$ $\delta p_p = 0$

t_{ul}	t_{us}	t_{dl}	t_{ds}
1672	2373	1680	2383
1672	2373	1680	2385
1672	2373	1680	2388
1672	2373	1680	2385
1670	2370	1686	2389
1672	2372	1683	2384
1672	2372	1681	2386

Point J

$T_D = 80$ $T_W = 64$ $P_B = 30.44$ $\Delta p_o = 8.15$

$\delta p_o = 1.5$ $\delta p_p = .86$

t_{ul}	t_{us}	t_{dl}	t_{ds}
1707	2440	1645	2348
1704	2441	1648	2351
1708	2440	1646	2353
1704	2439	1642	2352
1707	2440	1647	2352
1705	2436	1644	2351
1708	2440	1642	2351
1704	2434		

Point K

$T_D = 77$ $T_W = 64$ $P_B = 30.44$ $\Delta p_o = 0$

$\delta p_o = 0$ $\delta p_p = 0$

t_{ul}	t_{us}	t_{dl}	t_{ds}
1680	2397	1662	2381
1680	2397	1663	2383
1678	2394	1664	2384
1679	2396	1659	2378
1679	2396	1663	2382
1681	2399	1663	2383
1678	2398	1665	2385

Appendix References

[1] *Annubar Flow Handbook*
Dietrich Standard Corporation, 1980.

[2] Bean, Howard S.
Fluid Meters, Their Theory and Application.
Technical Report 6, American Society of Mechanical Engineers, 1971.

[3] Britton, Charles.
Telephone conversations with author.
1982.

[4] Continos, Costas.
Information on large volume flow measurement presented at review meeting.
Jan, 1982.

[5] Fitzgerald, Kevin.
Development of a Curb Flowmeter.
Master's thesis, MIT, 1982.
Contains discussion of vortex shedding phenomena.

[6] Gooberman, G. L.
Ultrasonics Theory and Application.
Hart Publishing Co., New York, 1968.

[7] Hickman, William.
Annubar Properties Investigation.
In *Advances in Instrumentation.* ISA Industry Oriented Conference and Exhibit, October, 1975.

[8] Mason and Thurston (editor).
Ultrasonic Flowmeters.
Academic Press, 1979.

[9] McShane, J.L.
Ultrasonic Flowmeters.
In *Advances in Instrumentaion.* ISA International Instrumentation and Automation Conference, Oct, 1974.

[10] Munk, W. D.
The Ultrasonic Flowmeter - A New Approach to Large Volume Gas Measurement.
Presented at the Forty - First Appalachian Gas Measurement Course; Robert Morris College, Coraopolis, Pa. 1981.

[11] Pederson, Bradshaw, Lynnworth, and Morel.
New Ultrasonic Flowmeter for the Natural Gas Industry.
In *Proceedings of the Symposium on Flow Measurement in Open Channels and Closed Conduits.* NBS, 1977.